Math. Model. Nat. Phenom. 21 (2026) 21
https://doi.org/10.1051/mmnp/2026013

Mathematical Modelling of Natural Phenomena
www.mmnp-journal.org

EQUIVARIANT HOPF BIFURCATION OF A TIME-DELAYED REACTION-TAXIS-DIFFUSION PLANKTON MODEL WITH SELECTIVE GRAZING AND CANNIBALISM ON A CIRCULAR DOMAIN

Yiping Yang[1], Xiaofeng Xu[2] and Ming Liu[1,*]

Abstract. In this paper, we study a model about non-toxic phytoplankton (NTP), toxin-producing phytoplankton (TPP), and zooplankton defined on a two-dimensional circular domain with predator-taxis and time-delay. The relationship between NTP, TPP and zooplankton is explored by combining selective grazing, cannibalism, Allee effect and additional food. For the proposed model, a rigorous proof of global solution existence with uniform boundedness is provided. By applying the Brouwer fixed-point theorem, we demonstrate the existence of a positive constant steady-state solution. Within the functional analytic framework, we establish conditions for both standard and equivariant Hopf bifurcations occurring in the neighborhood of the spatially homogeneous equilibrium. Next we obtain the existence condition and specific properties of periodic solutions by bifurcation theory and normal form method. Numerically, we select appropriate parameters with practical significance and validate analytical predictions *via* computational experiments. Specifically, we show different types of rotating waves and standing waves, which are the rather complex dynamic behaviors in the two-dimensional circular domain. And then we reveal the periodic phenomena of NTP, TPP and zooplankton, as well as biological phenomena caused by selective grazing, cannibalism, Allee effect and additional food, which provides valuable results for monitoring and controlling the distribution of plankton populations and protecting aquatic ecosystems.

Mathematics Subject Classification. 37G05, 37G40, 34K20, 34K18, 92D25.

Received June 7, 2025. Accepted April 17, 2026.

1. Introduction

Plankton populations play a vital role in the aquatic ecosystem, especially in water quality regulation and material circulation. Plankton populations interact with each other to maintain the balance and function of the aquatic ecosystem [1, 2]. The predation relationship between zooplankton and phytoplankton serves an essential function, and in fact, zooplankton show a preference for specific foods when feeding on phytoplankton (such as

Keywords and phrases: Plankton selective grazing, predator-taxis, two-dimensional circular domain, standing wave and Rotating wave.

[1] Department of Mathematics, Northeast Forestry University, Harbin, Heilongjiang 150040, PR China.
[2] Engineering Research Center of Agricultural Microbiology Technology, Ministry of Education & Heilongjiang Provincial Key Laboratory of Ecological Restoration and Resource Utilization for Cold Region & School of Mathematical Science, Heilongjiang University, Harbin 150080, PR China.

* Corresponding author: liuming_girl@163.com

© The authors. Published by EDP Sciences, 2026

This is an Open Access article distributed under the terms of the Creative Commons Attribution License (https://creativecommons.org/licenses/by/4.0), which permits unrestricted use, distribution, and reproduction in any medium, provided the original work is properly cited.

plankton algae) or other tiny organic matter, rather than randomly choosing foods. This way of selective grazing is part of a complex interaction between zooplankton and their environment that has important implications for the energy flow of ecosystems and competition between species [3–5]. Zooplankton selective grazing can also be divided into several categories based on its characteristics, such as nutrient preferences [6], and zooplankton often choose phytoplankton or organic particles with higher nutritional value. Zooplankton may choose the size of food to avoid eating too large or too small particles [7–9]. Additionally, zooplankton have species selectivity among many kinds of phytoplankton and algae [10]. As well as selection according to the chemical properties of food, some zooplankton are able to detect chemical signals of food and thus select specific species of phytoplankton [11, 12]. For example, some zooplankton can make choices by sensing the presence of certain chemicals to determine the nutritional status or toxicity of algae. This kind of selective grazing for toxicity has attracted wide attention in recent years, specifically refers to the behavior of zooplankton avoidance of toxic phytoplankton (TPP) or selective feeding of non-toxic phytoplankton (NTP) when feeding [13–16].

From an ecological point of view, in aquatic ecosystems, many phytoplankton, especially some algae, may produce toxic substances under environmental pressures (such as eutrophication, rising water temperatures, changes in light, *etc.*), which are harmful to aquatic animals. For example, cyanobacteria (such as microcystis) can secrete toxins (such as microcystis) that are lethal to zooplankton and other aquatic life. Their outbreaks usually occur in eutrophic waters, where there is an excess of nutrients (especially nitrogen and phosphorus), toxic algae tend to multiply rapidly and form blooms [17–19]. Blooms not only affect water quality, but also cause water hypoxia, ecosystem imbalance, and even damage fishery resources. Thus, selective grazing of toxic phytoplankton by plankton contributes significantly to water management, especially in controlling toxic algal outbreaks. By avoiding the feeding of toxic algae, zooplankton can reduce the spread of toxic algae and thus mitigate their negative impact on the overall ecosystem, especially in water bodies with frequent toxic algae outbreaks, the selective grazing behavior of zooplankton helps to maintain ecosystem stability [20].

From a mathematical point of view, the complex dynamic processes of the plankton system have always been a research focus, many scholars have established nonlinear mathematical models to study aquatic ecosystems and complex relationships among various types of plankton [21–24]. Apart from that there are many studies on the interaction among NTP, TPP and zooplankton, of which Roy *et al.* [25] constructed and analyzed a mathematical model of zooplankton preference for NTP and avoidance of TPP. The study showed that the existence of high avoidance is conducive to the initiation of blooms by toxic phytoplankton species. Chakraborty *et al.* [26] introduced the selective grazing into models incorporating these three populations. Not only does selective grazing foster species coexistence, but more importantly, systematic scenario simulations of ecological processes prove its essential role in securing TPP's survival advantage within competitive ecosystems. The study in [26] employs a mathematical framework with $P(x,t)$, $H(x,t)$ and $Z(x,t)$ quantifying the local densities of NTP, TPP and zooplankton at any given point x and moment t , which is as follows.

$$\begin{cases} \dfrac{\mathrm{d}P}{\mathrm{d}t} = r_1 P\left(1-\dfrac{P}{K_1}\right) - a_1 PH - \dfrac{b_1 PZ}{c_1+P}, \\ \dfrac{\mathrm{d}H}{\mathrm{d}t} = r_2 H\left(1-\dfrac{H}{K_2}\right) - a_2 PH - \dfrac{b_2 HZ}{c_2+\theta_1 P+H}, \\ \dfrac{\mathrm{d}Z}{\mathrm{d}t} = \dfrac{e_1 PZ}{c_1+P} - \dfrac{e_2 HZ}{c_2+\theta_1 P+H} - d_1 Z. \end{cases} \tag{1.1}$$

In fact, because the toxins released by the TPP will cause the rapid death of zooplankton, zooplankton must have additional food (bacteria, food debris, and smaller zooplankton) to survive [27]. By ingesting additional food sources, zooplankton can effectively adapt to these unstable environmental conditions to maintain survival and reproduce, which is an effective species conservation strategy [28]. Besides, another self-protection mechanism of zooplankton is cannibalism, in which larger individuals prey on smaller members of the same species or eat eggs, larvae and so on, in order to provide themselves with needed energy [29]. This also maintains the stability and energy flow of the ecosystem to a certain extent, however, excessive cannibalism can also lead to the extinction

of zooplankton populations and even the loss of biodiversity of the populations [30]. Furthermore, the Allee effect is also a common phenomenon in biological populations, especially plankton populations, which describes the decline in reproductive success of certain species at low densities [31–33].

Moreover, when explaining practical problems, the non-spatial models constructed by ordinary differential equations often have limitations and may not reflect the real phenomena more truly. As far as aquatic ecology is concerned, plankton exists in ocean and rivers. Due to the mobility of water, the distribution of plankton in different spatial locations will be uneven, consequently, spatial dependencies need to be incorporated into the framework. The reference [34] introduces the diffusion into the model (1.1) and considers the selective grazing in a heterogeneous environment. Then the following model is established and the existence of Turing instability and nonconstant positive steady states in one-dimensional space is analyzed.

$$\begin{cases} \dfrac{\partial P}{\partial t} = r_1 P\left(1-\dfrac{P}{K_1}\right) - a_1 PH - \dfrac{b_1 PZ}{c_1+P+\alpha\beta A} + D_1\Delta P, \\ \dfrac{\partial H}{\partial t} = r_2 H\left(1-\dfrac{H}{K_2}\right) - a_2 PH - \dfrac{b_2 HZ}{c_2+\theta_1 P+\theta_2 H^2} + D_2\Delta H, \\ \dfrac{\partial Z}{\partial t} = \dfrac{Z}{\delta+Z}\left(\dfrac{e_1(P+\beta A)Z}{c_1+P+a\beta A} - \dfrac{e_2 HZ}{c_2+\theta_1 P+\theta_2 H^2}\right) - d_1 Z - d_2 Z^2 \\ \qquad + D_3\Delta Z - \nabla\cdot(\chi_1 Z\nabla P) + \nabla\cdot(\chi_2 Z\nabla H). \end{cases}$$

In fact, in addition to considering the effect of space, that is, introducing the diffusion term, it is also necessary to consider the time-delay term. Many time-delay models have been established to describe plankton populations. Medvinsky *et al.* [35] found that time delay can gradually replace regular plankton dynamics through bifurcations and chaos. In addition, there are other reasons for the delay of population dynamics at different time scales [36–40]. More than that, plankton is distributed in marine or lakes, which can be more realistically abstracted as a two-dimensional circular plane. Compared with the one-dimensional space, considering the dynamic behavior of the plankton population model on the two-dimensional circular domain is not only closer to reality from the biological point of view, but also more practical significance. From a mathematical point of view, on a two-dimensional circular domain, there exist multiple pure imaginary eigenvalues because of the O(2) symmetry. In this case, the Laplacian eigenspace is two-dimensional, which leads to the emergence of a high-dimensional central subspace at the bifurcation points. Consequently, the related dynamic behavior of the dynamic system on the circular domain will be more complex. For example, it may produce spatially inhomogeneous periodic solutions such as rotating waves, standing waves, spatially homogeneous periodic solutions and more complex patterns [41, 42].

The periodic solution reflects the periodic phenomenon of plankton population, which is of great significance in ecology. Periodic fluctuations of plankton populations reflect dynamic changes of energy flow in the ecosystem [43–45]. Understanding this periodicity can help predict the stability and health of ecosystems. Periodical changes in plankton populations can also encourage different species to occupy ecological niches at different times, avoiding excessive competition and helping to maintain biodiversity. Periodic fluctuations can sometimes promote the outbreak of certain species in a specific period, driving changes in the species structure of the ecosystem. Moreover, the periodic phenomenon of plankton population is also very sensitive to changes in environmental factors (such as temperature, light, nutrient concentration, *etc.*). By studying such periodic changes, we can reveal the impact of climate change on aquatic ecosystems, and provide data support for climate monitoring and prediction. Changes in plankton populations often also reflect the nutrient status of the water (such as eutrophication), and the regularity of periodic changes helps to identify early signs of water pollution or ecological imbalance [46–48]. In general, the periodic phenomenon of plankton population is of great significance in the fields of ecology, environmental science, fisheries resource management and climate change research. Strengthening the study and monitoring of plankton population periodic phenomenon is crucial for protecting the aquatic ecosystem, promoting the sustainable use of fishery resources, coping with climate change and promoting the development of related scientific research and technology.

Different from [34], adding the influence of the time delay term, in this paper we discuss the dynamic behavior of the NTP–TTP–zooplankton model on the two-dimensional circular domain and focus on the periodic solutions of the system, so as to reveal the periodic phenomena among NTP, TTP and zooplankton reflected by these periodic solutions and the biological significance behind them, such as the specific description and embodiment of enrichment paradox. The specific form of the model is as follows.

$$\begin{cases} \dfrac{\partial P}{\partial t} = D_1\Delta P + r_1 P\left(1-\dfrac{P}{K_1}\right) - a_1 PH - \dfrac{b_1 PZ}{c_1 + a\beta A + P}, & (r,\theta)\in\Omega,\ t>0,\\ \dfrac{\partial H}{\partial t} = D_2\Delta H + r_2 H\left(1-\dfrac{H}{K_2}\right) - a_2 PH - \dfrac{b_2 HZ}{c_2 + \theta_1 P + \theta_2 H^2}, & (r,\theta)\in\Omega,\ t>0,\\ \dfrac{\partial Z}{\partial t} = D_3\Delta Z - \nabla\cdot(\chi_1 Z\nabla P) + \nabla\cdot(\chi_2 Z\nabla H) & \\ \qquad + \dfrac{Z^2}{\delta+Z}\left(\dfrac{e_1(P_\tau+\beta A)}{c_1+P_\tau+a\beta A} - \dfrac{e_2 H_\tau}{c_2+\theta_1 P_\tau+\theta_2 H_\tau^2}\right) - d_1 Z - d_2 Z^2, & (r,\theta)\in\Omega,\ t>0, \end{cases} \tag{1.2}$$

with initial conditions and boundary conditions

$$\begin{cases} \dfrac{\partial P}{\partial \nu} = \dfrac{\partial H}{\partial \nu} = \dfrac{\partial Z}{\partial \nu} = 0, & (r,\theta)\in\partial\Omega,\ t>0,\\ P(r,\theta,0) = P_0(r,\theta) \geq (\not\equiv)\, 0,\\ H(r,\theta,0) = H_0(r,\theta) \geq (\not\equiv)\, 0,\\ Z(r,\theta,0) = Z_0(r,\theta) \geq (\not\equiv)\, 0, & (r,\theta)\in\Omega, \end{cases}$$

where $\Omega = \{(r,\theta) : 0\leq r\leq R,\ 0\leq\theta\leq 2\pi\}$, $P_\tau = P(r,\theta,t-\tau)$, $H_\tau = H(r,\theta,t-\tau)$ and ν is normal outward vector, r_1 and r_2 are the intrinsic growth rates of NTP and TPP populations, respectively; K_1 and K_2 are the carrying capacities of NTP and TPP populations, respectively; a_1 and a_2 measure the inter-specific competitive effect of TPP and NTP respectively; b_1 and b_2 are the consumption or predation rates of NTP and TPP, respectively; c_1 and c_2 are the half saturation constants of NTP and TPP, respectively; α is the quality of additional food; β is the relative ability of zooplankton to detect additional food; A is the amount of additional food; θ_1 is the preference coefficient; θ_2 is the avoidance coefficient; δ is the intensity of the Allee effect; e_1 is the maximal conversion rate from individuals of NTP into individuals of zooplankton; e_2 is the death rate of zooplankton due to predation of TPP; d_1 is the mortality rate of zooplankton; d_2 is the cannibalism rate among zooplankton; $D_1,\ D_2,\ D_3$ is the self-diffusion coefficient of NTP, TTP and zooplankton, respectively; χ_1 is the coefficient reflecting the chasing effect of zooplankton on NTP; χ_2 is the coefficient reflecting the toxin avoidance effect of zooplankton on TPP.

In contrast to earlier studies, our research in this paper has several new features, as outlined below. Our study investigates a plankton model on a two-dimensional circular domain, where lakes or oceanic environments are abstracted as a circular disk—an approach that undeniably holds greater practical relevance. While most existing research focuses on one-dimensional spatial frameworks, and only a limited number of studies characterize population dynamics on two-dimensional rectangular domains, explorations in circular domains remain exceptionally scarce. In reality, the inherent symmetry of circular domains induces higher-dimensional central subspaces at bifurcation points, leading to more intricate dynamical behaviors in such systems, as robustly demonstrated by our results. Theoretically, analyzing system dynamics in circular domains presents greater challenges compared to one-dimensional cases. Spatial decomposition and the derivation of characteristic equations necessitate the integration of Bessel function theory, diverging from the trigonometric function-based approaches applicable in one-dimensional analyses. Furthermore, this work examines a three-species plankton model, rigorously establishing the existence and boundedness of solutions while calculating normal forms through bifurcation theory. These tasks entail significantly higher computational complexity compared to two-species models, reflecting the heightened challenges of this investigation. However, to address these challenges,

we adopted innovative methodologies. For example, in proving the existence of a positive equilibrium for the system (1.2), our approach diverges from conventional techniques that rely on direct algebraic computation. Instead, we constructed a compact convex set and applied Brouwer fixed-point theorem to establish the existence of solutions. This strategy circumvents the analytical complexities inherent in directly solving nonlinear equations while rigorously ensuring the theoretical existence of equilibria.

The rest of the paper proceeds with the following structure. In Section 2, we establish the global existence and boundedness of the solutions of the system without delay by using the comparison principle and a prior estimation. In Section 3, we prove the existence of the positive equilibrium point of the system (1.2) using the Brouwer fixed-point theorem by constructing a compact convex set. Besides, the conditions for the existence of Hopf bifurcation and equivariant Hopf bifurcation are given by the bifurcation theory, and the direction and stability of bifurcations are given by the normal form method. In Section 4, through numerical simulations, we aim to validate our theoretical predictions and explore spatially homogeneous and non-homogeneous periodic wave patterns, specifically examining rotating waves and standing waves. The conclusions of this paper will be summarized in Section 5. In this paper, we use $\|\cdot\|_{\boldsymbol{p}}$ as the norm of $L^p(\Omega)$, $1 \le p \le \infty$; $\|\cdot\|_{m,k}$ as the norm of $W^{m,k}(\Omega)$, $m = 1, 2$; $1 \le k \le \infty$. We define that a function v belonging to $C^{3,1}(\bar{\Omega}(0, T_{max}))$ possesses continuous partial derivatives up to third order in the spatial variables $x \in \bar{\Omega}$ and up to first order in the time variable $t \in (0, T_{max})$. And in the following article without confusion, we abbreviate $\int_\Omega \cdot \, \mathrm{d}x$ as $\int_\Omega \cdot$ for simplicity.

2. Global existence and boundedness

This section rigorously demonstrates the global boundedness and existence of solutions of the system without delay for arbitrary spatial dimensions. By applying Amann's abstract theory for the quasilinear parabolic system in [49, 50], we present the following theorem, which establishes the local-in-time existence of classical solutions.

Lemma 2.1. *Let Ω be a bounded domain in $\mathbb{R}^n (n \ge 1)$ with smooth boundary $\partial\Omega$. Assume that $(P_0, H_0, Z_0) \in \left(W^{1,p}(\Omega)\right)^3$ for some $p > n$ with $P_0, H_0, Z_0 \ge 0 \, (\not\equiv 0)$. Then there exists a constant $T_{\max} \in (0, \infty]$ such that system (1.2) admits a unique classical solution $(P(x,t), H(x,t), Z(x,t))$ satisfying $P, H, Z > 0$ for all $t > 0$, and $(P, H, Z) \in \left(C\left([0, T_{\max}); \ W^{1,p}(\Omega)\right) \cap C^{3,1}\left(\bar{\Omega} \times (0, T_{\max})\right)\right)^3$. Moreover, either $T_{\max} = \infty$ or $\|P(\cdot,t)\|_{L^\infty} + \|H(\cdot,t)\|_{L^\infty} + \|Z(\cdot,t)\|_{L^\infty} \to \infty$ as $t \to T_{\max}$.*

Next, we present the boundedness analysis of $P(x,t)$, $H(x,t)$ and the L^1 estimate for $Z(x,t)$.

Lemma 2.2. *Under the assumptions in Lemma 2.1, there exist positive constants C_1, C_2, C_3 such that, the solution (P, H, Z) of the system (1.2) satisfies*

$$0 < P(x,t) \le C_1 := \max\left\{\|P_0\|_{L^\infty}, K_1\right\}, \ \text{for all } x \in \Omega, \ t > 0, \tag{2.1}$$

$$0 < H(x,t) \le C_2 := \max\left\{\|H_0\|_{L^\infty}, K_2\right\}, \ \text{for all } x \in \Omega, \ t > 0, \tag{2.2}$$

$$\int_\Omega Z(x,t)\,\mathrm{d}x \le C_3 := \max\left\{|\Omega|(C_1 + \beta A)/d_2, \|Z_0\|_1\right\}, \ \text{for all} t \in (0, T_{\max}). \tag{2.3}$$

Proof. To prove, from the nonnegativity of P, H, Z, we have

$$\begin{cases} P_t = D_1\Delta P + r_1 P\left(1 - \dfrac{P}{K_1}\right) - a_1 PH - \dfrac{b_1 PZ}{c_1 + a\beta A + P} \le D_1\Delta P + r_1 P\left(1 - \dfrac{P}{K_1}\right), & x \in \Omega, t > 0, \\ \dfrac{\partial P}{\partial \nu} = 0, & x \in \partial\Omega, t > 0, \\ P(x,0) = P_0(x), & x \in \Omega. \end{cases} \tag{2.4}$$

Let $P_*(t)$ be the solution of the following ODE problem

$$\begin{cases} \dfrac{\mathrm{d}}{\mathrm{d}t}P_*(t) = r_1 P_*(t)\left(1-\dfrac{P_*(t)}{K_1}\right), \ t>0, \\ P_*(0) = \|P_0\|_{L^\infty}. \end{cases} \tag{2.5}$$

It is easy to see that $P_*(t) \le C_1 := \max\{\|P_0\|_{L^\infty}, K_1\}$. Thus, $P_*(t)$ is a super-solution of the following PDE problem

$$\begin{cases} \hat{P}_t = D_1\Delta\hat{P} + r_1\hat{P}\left(1-\dfrac{\hat{P}}{K_1}\right), & x\in\Omega, \ t>0, \\ \dfrac{\partial\hat{P}}{\partial\nu} = 0, & x\in\partial\Omega, \ t>0, \\ \hat{P}(x,0) = P_0(x), & x\in\Omega. \end{cases} \tag{2.6}$$

We then obtain

$$0 < \hat{P}(x,t) \le P_*(t), \ \text{for all } (x,t)\in\bar{\Omega}\times(0,\infty), \tag{2.7}$$

where the inequality $\hat{P}(x,t) > 0$ follows directly from the application of the strong maximum principle.

Applying the comparison principle, from (2.4), (7) and (2.7), we obtain

$$0 < P(x,t) \le \hat{P}(x,t) \le P_*(t) \le C_1, \ \text{for all } (x,t)\in\bar{\Omega}\times(0,\infty),$$

thus we obtain the result (2.1), for the same way, we can prove (2.2).

Let

$$S(t) = \int_\Omega Z(x,t)\,\mathrm{d}x, \quad F^{(3)}(P,H,Z) = \frac{Z}{\delta+Z}\left(\frac{e_1(P+\beta A)Z}{c_1+P+a\beta A} - \frac{e_2HZ}{c_2+\theta_1P+\theta_2H^2}\right) - d_1Z - d_2Z^2,$$

then

$$\begin{aligned} \frac{\partial S(t)}{\partial t} &= \int_\Omega [D_3\Delta Z - \nabla\cdot(\chi_1 Z\nabla P) + \nabla\cdot(\chi_2 Z\nabla H) + F^{(3)}(P,H,Z)]\,\mathrm{d}x \\ &= D_3\int_\Omega \frac{\partial Z}{\partial\nu}\,\mathrm{d}S - \chi_1\int_\Omega Z\frac{\partial P}{\partial\nu}\,\mathrm{d}S + \chi_2\int_\Omega Z\frac{\partial H}{\partial\nu}\,\mathrm{d}S + \int_\Omega F^{(3)}(P,H,Z)\,\mathrm{d}x \\ &= \int_\Omega F^{(3)}(P,H,Z)\,\mathrm{d}x \le \int_\Omega\left(\frac{e_1(P+\beta A)Z}{e_1+P+\alpha\beta A} - d_2Z^2\right)\mathrm{d}x \le \int_\Omega((C_1+\beta A)Z - d_2Z^2)\,\mathrm{d}x. \end{aligned}$$

Then we can get $\int_\Omega Z^2\,\mathrm{d}x \ge \left(\int_\Omega Z\,\mathrm{d}x\right)^2/|\Omega|$ by applying the Hölder inequality, thus we get

$$\frac{\partial S(t)}{\partial t} \le (\bar{C}_1+\beta A)S(t) - \frac{d_2}{|\Omega|}S^2(t),$$

which leads to (2.3).

In the following, we recall some preliminary estimates in [51], which will be crucial for establishing the global solvability of the system. Now we provide some estimates for the diffusion semigroup with homogeneous Neumann boundary conditions, which discussed in [51, 52].

First of all, for $p \in (1,\infty)$, the sectorial operator A is defined by $AP := -\Delta P$ for $P \in D(A) := \{\varphi \in W^{2,p}(\Omega) : \frac{\partial \varphi}{\partial \nu} = 0, \text{ on } \partial\Omega\}$. Similarly, A_d is defined by $A_{\mathrm{d}}P = -\mathrm{d}\Delta P$, which possesses the same properties as A due to a direct scaling, hence we only state the results on A here.

Lemma 2.3. *(1) Assume that $k \in \{0,1\}, 1 \le p \le \infty, 1 < q < \infty$. There exists a constant $c_1 > 0$, such that*

$$\|P\|_{k,p} \le c_1 \|(A+1)^{\theta} P\|_q, \tag{2.8}$$

for any $P \in D((A+1)^{\theta})$ with $0 < \theta < 1$ satisfying

$$k - \frac{n}{p} < 2\theta - \frac{n}{q}.$$

If additionally for any $u \in L^{q'}(\Omega), q \ge q'$, then there exists $c_2 > 0,\ r > 0$ such that

$$\|(A+1)^{\theta} \mathrm{e}^{-t(A+1)} P\|_q \le c_2 (t^{-\theta - \frac{n}{2}(\frac{1}{p}-\frac{1}{q})}) \mathrm{e}^{-rt} \|P\|_{q'}, \tag{2.9}$$

where $\mathrm{e}^{-t(A+1)}$ maps $L^{q'}$ into $D((A+1)^{\theta})$.

(2) For $1 < p < \infty$, there exist some positive constants $c_3, \epsilon > 0$ and μ, such that

$$\|(A+1)^{\theta} \mathrm{e}^{-tA} \nabla \cdot P\|_p \le c_3 (t^{-\theta - \frac{1}{2} - \epsilon}) \mathrm{e}^{-\mu t} \|P\|_p, \tag{2.10}$$

for all $P \in L^p$.

Analogous to Lemma 2.3, H yields a corresponding result. We subsequently invoke the Gagliardo-Nirenberg inequality (as documented in [53–55]) to establish the boundedness of $Z(x,t)$ in subsequent analyses.

Lemma 2.4. *There exists an constant $C_{GN} > 0$ such that*

$$\|u\|_p \le C_{GN} \|u\|_{1,q}^{\sigma} \|u\|_k^{1-\sigma}, \tag{2.11}$$

for $u \in W^{1,q}(\Omega)$, where $p \ge q \ge 1,\ p \ge k$ satisfy

$$\frac{nq(p-k)}{kpq + np(q-k)} \le \sigma \le 1,$$

with sharply inequality if $k = 1$ or $q = 1$.

Next, we give the L^{n+2} estimate of $Z(x,t)$ through weight functions $\varphi(P)$ and $\varphi(H)$ similar to that in [56].

Lemma 2.5. *Letting (P,H,Z) be the classical solution of the system over $(0,T_{\max})$ with χ_1, χ_2 satisfying*

$$0 < \chi_1 \le \frac{D_1 D}{5(n+2)(D_1+D_2+D_3)C}, \quad 0 < \chi_2 \le \frac{D_2 D}{5(n+2)(D_1+D_2+D_3)C}, \tag{2.12}$$

where $C = \max\{C_1, C_2\},\ D = \min\{D_1, D_2\}$, there exists a constant $R > 0$ such that for all $t \in (0, T_{\max})$, the following inequality holds,

$$\|Z(\cdot,t)\|_{L^{n+2}} \le R. \tag{2.13}$$

Proof. We begin by proving that for any $\tau \in (0, T_{\max})$, there exists a constant $G_1(\tau) > 0$ such that the following inequality holds

$$||P(\cdot,t)||_{1,\infty} \leq G_1(\tau), \text{ for all } t \in (\tau, T_{\max}).$$

Let $\tau \in (0, T_{\max})$ be chosen such that $\tau < 1$, and let $q = n + 2$ and $\theta \in \left(\frac{1}{2}(1 + \frac{n}{q}), 1\right)$. The first equation of (1.2) can be expressed in an alternative form as

$$\frac{\partial P}{\partial t} = D_1 \Delta P - P + \varphi(P, H, Z), \tag{2.14}$$

where $\varphi(P,H,Z) = P\left(r_1 + 1 - \frac{r_1}{K_1}P - a_1 H - \frac{b_1 Z}{c_1 + P + \alpha\beta A}\right)$. Now, applying the variation of constants formula to (2.14), we have

$$P(\cdot,t) = \mathrm{e}^{-t(A_{D_1}+1)}P_0 + \int_0^t \mathrm{e}^{-(t-s)(A_{D_1}+1)}\varphi(P(\cdot,t), H(\cdot,t), Z(\cdot,t))\mathrm{d}s.$$

By referring to (2.8) and (2.9) in Lemma 2.3, for all $t \in (\tau, T_{\max})$, it follows that

$$\begin{aligned}
||P(\cdot,t)||_{1,\infty} &\leq K||(A_{D_1}+1)^{\theta}P(\cdot,t)||_q \leq K\int_0^t (t-s)^{-\theta}\mathrm{e}^{-\gamma(t-s)}||\varphi(P,H,Z)||_q ds + Kt^{-\theta}\mathrm{e}^{-\gamma t}||P_0||_q \\
&\leq K\int_0^t (t-s)^{-\theta}\mathrm{e}^{-\gamma(t-s)}||P(\cdot,t)||_{\infty}\mathrm{d}s + Kt^{-\theta}\mathrm{e}^{-\gamma t}||P_0||_q \leq Kt^{-\theta} + K\int_0^t (t-s)^{-\theta}\mathrm{e}^{-\gamma(t-s)}\mathrm{d}s \\
&\leq Kt^{-\theta} + K\int_0^{\infty} \sigma^{-\theta}\mathrm{e}^{-\gamma\sigma}\mathrm{d}\sigma \leq K(\tau^{-\theta}+1) := G_1(\tau).
\end{aligned}$$

By the same way, for any $\tau \in (0, T_{\max})$, we can deduce the existence of a constant $G_2(\tau) > 0$ such that for all $t \in (\tau, T_{\max})$, we obtain the following

$$||H(\cdot,t)||_{1,\infty} \leq G_2(\tau).$$

At this stage, we formally introduce the constants

$$k := n + 2, \ \eta := \sqrt{\frac{k-1}{10k}} \cdot \frac{D}{(D_1 + D_2 + D_3)C}, \tag{2.15}$$

and a weight function

$$\varphi(P) := \mathrm{e}^{(\eta P)^2}, \ 0 \leq P \leq C_1,$$

then we have

$$1 \leq \varphi(P) \leq \mathrm{e}^{(\eta C_1)^2} := h_1 > 1, \ 0 \leq P \leq C_1. \tag{2.16}$$

From (1.2) and Young's inequality, we acquire

$$\begin{aligned}
&\frac{1}{k}\frac{\mathrm{d}}{\mathrm{d}t}\int_\Omega Z^k\varphi(P) = \int_\Omega Z^{k-1}\varphi(P)Z_t + \frac{1}{k}\int_\Omega Z^k\varphi'(P)P_t\\
&\le \int_\Omega Z^{k-1}\varphi(P)D_3\Delta Z - \int_\Omega Z^{k-1}\varphi(P)\chi_1\nabla\cdot(Z(\nabla P) + \int_\Omega Z^{k-1}\varphi(P)\chi_2\nabla\cdot(Z(\nabla H)\\
&+ \int_\Omega Z^{k-1}\varphi(P)F^{(3)} + \frac{D_1}{k}\int_\Omega Z^k\varphi'(P)\Delta P + \frac{1}{k}\int_\Omega Z^k\varphi'(P)(-P+\varphi(P,H,Z))\\
&\le -(k-1)D_3\int_\Omega Z^{k-2}\varphi(P)|\nabla Z|^2 - D_3\int_\Omega Z^{k-1}\varphi'(P)\nabla Z\nabla P + \chi_1\int_\Omega Z^{k-1}Z\varphi'(P)|\nabla P|^2\\
&+ \chi_1(k-1)\int_\Omega Z^{k-2}Z\varphi(P)\nabla P\nabla Z - \chi_2\int_\Omega Z^{k-1}Z\varphi'(P)|\nabla H|^2 - \chi_2(k-1)\int_\Omega Z^{k-2}Z\varphi(P)\nabla H\nabla Z\\
&+ \int_\Omega Z^k\varphi(P) - D_1\int_\Omega Z^{k-1}\varphi'(P)\nabla P\nabla Z - \frac{D_1}{k}\int_\Omega Z^k\varphi''(P)|\nabla P|^2 + 2\eta^2\frac{K_1}{k}\int_\Omega Z^k\varphi(P)P^2.
\end{aligned}$$

Then, we have

$$\begin{aligned}
&\frac{1}{k}\frac{\mathrm{d}}{\mathrm{d}t}\int_\Omega Z^k\varphi(P) + (k-1)D_3\int_\Omega Z^{k-2}\varphi(P)|\nabla Z|^2 + \frac{D_1}{k}\int_\Omega Z^k\varphi''(P)|\nabla P|^2\\
&\le -(D_1+D_3)\int_\Omega Z^{k-1}\varphi'(P)\nabla Z\nabla P + \chi_1(k-1)\int_\Omega Z^{k-1}\varphi(P)\nabla P\nabla Z + \chi_2(k-1)\int_\Omega Z^{k-1}\varphi(P)\nabla H\nabla Z\\
&+ \chi_1\int_\Omega Z^k\varphi'(P)|\nabla P|^2 + \chi_2\int_\Omega Z^k\varphi'(P)|\nabla H|^2 + \int_\Omega Z^k\varphi(P) + 2\eta^2\frac{K_1}{k}\int_\Omega Z^k\varphi(P)P^2.
\end{aligned} \tag{2.17}$$

From Young's inequality, we obtain

$$-(D_1+D_3)\int_\Omega Z^{k-1}\varphi'(P)\nabla Z\nabla P \le \frac{D_1(k-1)}{4}\int_\Omega Z^{k-2}\varphi(P)|\nabla Z|^2 + \frac{(D_3+D_1)^2}{D_1(k-1)}\int_\Omega Z^k\frac{\varphi'^2(P)}{\varphi(P)}|\nabla P|^2, \tag{2.18}$$

$$\chi_1(k-1)\int_\Omega Z^{k-1}\varphi(P)\nabla P\nabla Z \le \frac{D_1(k-1)}{4}\int_\Omega Z^{k-2}\varphi(P)|\nabla Z|^2 + \frac{\chi_1^2(k-1)}{D_1}\int_\Omega Z^k\varphi(P)|\nabla P|^2, \tag{2.19}$$

$$\chi_2(k-1)\int_\Omega Z^{D_1(k-1)}\varphi(P)\nabla H\nabla Z \le \frac{D_1(k-1)}{4}\int_\Omega Z^{k-2}\varphi(P)|\nabla Z|^2 + \frac{\chi_2^2(k-1)}{D_1}\int_\Omega Z^k\varphi(P)|\nabla H|^2. \tag{2.20}$$

Substituting (2.18), (2.19) and (2.20) into (2.17), we have

$$\begin{aligned}
&\frac{1}{k}\frac{\mathrm{d}}{\mathrm{d}t}\int_\Omega Z^k\varphi(P) + \frac{D_1(4D_3-3)(k-1)}{4}\int_\Omega Z^{k-2}\varphi(P)|\nabla Z|^2 + \frac{D_1}{k}\int_\Omega Z^k\varphi''(P)|\nabla P|^2\\
&\le \frac{(D_3+D_1)^2}{D_1(k-1)}\int_\Omega Z^k\frac{\varphi'^2(P)}{\varphi(P)}|\nabla P|^2 + \frac{\chi_1^2(k-1)}{D_1}\int_\Omega Z^k\varphi(P)|\nabla P|^2 + \frac{\chi_2^2(k-1)}{D_1}\int_\Omega Z^k\varphi(P)|\nabla H|^2\\
&+ \frac{\chi_1}{D_1}\int_\Omega Z^k\varphi'(P)|\nabla P|^2 + \frac{\chi_2}{D_1}\int_\Omega Z^k\varphi'(P)|\nabla H|^2 + \int_\Omega Z^k\varphi(P) + 2\eta^2\frac{K_1}{k}\int_\Omega Z^kP^2\varphi(P)\\
&:= J_1+J_2+J_3+J_4+J_5+J_6+J_7.
\end{aligned} \tag{2.21}$$

Then we define another weight function $\varphi(H) := \mathrm{e}^{(\eta H)^2},\ 0 \le H \le C_2$, where k and η is the same as (2.15) and we have

$$1 \le \varphi(H) \le \mathrm{e}^{(\eta C_2)^2} := h_2 > 1,\ 0 \le H \le C_2. \tag{2.22}$$

By the same way, we obtain the following inequality,

$$\begin{aligned}
&\frac{1}{k}\frac{\mathrm{d}}{\mathrm{d}t}\int_\Omega Z^k\varphi(H) + \frac{D_2(4D_3-3)(k-1)}{4}\int_\Omega Z^{k-2}\varphi(H)|\nabla Z|^2 + \frac{D_2}{k}\int_\Omega Z^k\varphi''(H)|\nabla H|^2\\
&\le \frac{(D_3+D_2)^2}{D_2(k-1)}\int_\Omega Z^k\frac{\varphi'^2(H)}{\varphi(H)}|\nabla H|^2 + \frac{\chi_1^2(k-1)}{D_2}\int_\Omega Z^k\varphi(H)|\nabla P|^2 + \frac{\chi_2^2(k-1)}{D_2}\int_\Omega Z^k\varphi(H)|\nabla H|^2\\
&+ \frac{\chi_1}{D_2}\int_\Omega Z^k\varphi'(H)|\nabla P|^2 + \frac{\chi_2}{D_2}\int_\Omega Z^k\varphi'(H)|\nabla H|^2 + \int_\Omega Z^k\varphi(H) + 2\eta^2\frac{K_1}{k}\int_\Omega Z^k H^2\varphi(H)\\
&:= J_8 + J_9 + J_{10} + J_{11} + J_{12} + J_{13} + J_{14},
\end{aligned} \tag{2.23}$$

add (2.21) and (2.23) together,

$$\begin{aligned}
&\frac{1}{k}\frac{\mathrm{d}}{\mathrm{d}t}\int_\Omega Z^k\varphi(P) + \frac{1}{k}\frac{\mathrm{d}}{\mathrm{d}t}\int_\Omega Z^k\varphi(H) + \frac{D_1(4D_3-3)(k-1)}{4}\int_\Omega Z^{k-2}\varphi(P)|\nabla Z|^2\\
&+ \frac{D_2(4D_3-3)(k-1)}{4}\int_\Omega Z^{k-2}\varphi(H)|\nabla Z|^2 + \frac{D_1}{k}\int_\Omega Z^k\varphi''(P)|\nabla P|^2 + \frac{D_2}{k}\int_\Omega Z^k\varphi''(H)|\nabla H|^2\\
&\le J_1 + J_2 + J_3 + J_4 + J_5 + J_6 + J_7 + J_8 + J_9 + J_{10} + J_{11} + J_{12} + J_{13} + J_{14}.
\end{aligned} \tag{2.24}$$

Next we do some computations to show that the terms J_1, J_2, J_4, J_8 and J_{10} on the right-hand side of (2.24) are dominated by $\frac{D_1}{k}\int_\Omega Z^k\varphi''(P)|\nabla P|^2$.

For $s \ge 0$, define

$$\begin{aligned}
&Q_1(s) = 4\frac{(D_3+D_1)^2}{D_1(k-1)}\eta^4 s^2\varphi(s), \quad Q_2(s) = Q_3(s) = \frac{\chi_1^2(k-1)}{D_1}\varphi(s),\\
&Q_4(s) = Q_5(s) = 2\chi_1\eta^2 s\varphi(s), \quad Q_6(s) = 2\frac{D_1}{k}\eta^2\varphi(s) + 4\frac{D_1}{k}\eta^4 s^2\varphi(s).
\end{aligned}$$

By a direct calculation, we acquire that, for $0 \le s \le C$,

$$\frac{Q_1(s)}{\frac{1}{5}Q_6(s)} \le \frac{10k}{k-1}\frac{(D_3+D_1)^2}{D_1^2}(\eta s)^2 \le \frac{10k}{k-1}\frac{(D_3+D_1)^2}{D_1}(\eta C)^2 = 1, \tag{2.25}$$

$$\frac{Q_2(s)}{\frac{1}{5}Q_6(s)} \le \frac{5k(k-1)\chi_1^2}{2D_1^2\eta^2} \le \frac{5k(k-1)}{2D_1}\frac{10k(D_3+D_1)^2C^2}{(k-1)D_1^2}\frac{D^2}{5k^2C^2(D_1+D_2+D_3)^2} \le 1, \tag{2.26}$$

$$\frac{Q_4(s)}{\frac{1}{5}Q_6(s)} \le \frac{5ks\chi_1}{D_1} \le \frac{5kC}{D_1}\frac{D_1D}{5k\left(D_1+D_2+D_3\right)C} = \frac{D}{D_1+D_2+D_3} < 1. \tag{2.27}$$

From (2.25), (2.26) and (2.27), we obtain that

$$\begin{aligned}&\frac{(D_3+D_1)^2}{D_1(k-1)}\int_\Omega Z^k\frac{\varphi'^2(P)}{\varphi(P)}|\nabla P|^2+\frac{\chi_1^2(k-1)}{D_1}\int_\Omega Z^k\varphi(P)|\nabla P|^2+\frac{\chi_1}{D_1}\int_\Omega Z^k\varphi'(P)|\nabla P|^2\\&+\frac{\chi_1^2(k-1)}{D_2}\int_\Omega Z^k\varphi(H)|\nabla P|^2+\frac{\chi_1}{D_2}\int_\Omega Z^k\varphi'(H)|\nabla P|^2\le\frac{D_1}{k}\int_\Omega Z^k\varphi''(P)|\nabla P|^2.\end{aligned}\tag{2.28}$$

Substituting (2.28) into (2.21), we obtain that

$$\frac{1}{k}\frac{\mathrm{d}}{\mathrm{d}t}\int_\Omega Z^k\varphi(P)+\frac{D_1(4D_3-3)(k-1)}{4}\int_\Omega Z^{k-2}\varphi(P)|\nabla Z|^2\le\left(1+\frac{2\eta^2C_1^2C}{k}\right)\int_\Omega Z^k\varphi(P).\tag{2.29}$$

It can be obtained by the same method of calculation and analysis that the terms J_3, J_5, J_7, J_9 and J_{11} on the right-hand side of (2.24) are dominated by $\frac{D_2}{k}\int_\Omega Z^k\varphi''(H)|\nabla H|^2$. Therefore, the following conclusions can be drawn,

$$\frac{1}{k}\frac{\mathrm{d}}{\mathrm{d}t}\int_\Omega Z^k\varphi(H)+\frac{D_2(4D_3-3)(k-1)}{4}\int_\Omega Z^{k-2}\varphi(H)|\nabla Z|^2\le\left(1+\frac{2\eta^2C_2^2C}{k}\right)\int_\Omega Z^k\varphi(H).\tag{2.30}$$

By applying Lemma 2.4, along with (2.3) and (2.16), we deduce that

$$\begin{aligned}\int_\Omega Z^k\varphi(P)\le h\int_\Omega Z^k&=h_1||Z^{\frac{k}{2}}||_2^2\le h_1C_3\left\|Z^{\frac{k}{2}}\right\|_{1,2}^{2\lambda}\left\|Z^{\frac{k}{2}}\right\|_{\frac{2}{k}}^{2(1-\lambda)}\le hC_3\left(C_4\left(\frac{k}{2}\right)\right)^{2\lambda}\left(\left\|\nabla Z^{\frac{k}{2}}\right\|_2+\left\|Z^{\frac{k}{2}}\right\|_{\frac{2}{k}}\right)^{2\lambda}\left\|Z^{\frac{k}{2}}\right\|_{\frac{2}{k}}^{2(1-\lambda)}\\&=hC_3\left(C_4\left(\frac{k}{2}\right)\right)^{2\lambda}\left(\left\|\nabla Z^{\frac{k}{2}}\right\|_2+\|Z\|_1^{\frac{2}{k}}\right)^{2\lambda}\|Z\|_1^{k(1-\lambda)}\le C_5\left(\left\|\nabla Z^{\frac{k}{2}}\right\|_2^2+1\right)^{\lambda},\end{aligned}\tag{2.31}$$

where $\lambda=\frac{kn-n}{2+kn-n}\in(0,1)$.

From (2.16) and (2.31), we obtain

$$\int_\Omega Z^{k-2}\varphi(P)|\nabla Z|^2\ge\int_\Omega Z^{k-2}|\nabla Z|^2=\frac{4}{k^2}\int_\Omega|\nabla Z^{\frac{k}{2}}|^2\ge\frac{4}{k^2C_5^{\frac{1}{\lambda}}}\left(\int_\Omega Z^k\varphi(P)\right)^{\frac{1}{\lambda}}-\frac{4}{k^2}.\tag{2.32}$$

Combining (2.29) and (2.32), we obtain

$$\frac{1}{k}\frac{\mathrm{d}}{\mathrm{d}t}\int_\Omega Z^k\varphi(P)\le-\frac{D_1(k-1)(4D_3-3)}{k^2C_5^{\frac{1}{\lambda}}}\left(\int_\Omega Z^k\varphi(P)\right)^{\frac{1}{\lambda}}+\frac{D_1(k-1)(4D_3-3)}{k^2}+\left(1+\frac{2\eta^2C_1^2C}{k}\right)\int_\Omega Z^k\varphi(P),\tag{2.33}$$

for all $t\in(0,T_{\max})$, where $\frac{1}{\lambda}>1$. Integrating (2.33), we obtain $\|Z(\cdot,t)\|_k\le\left(\int_\Omega Z^k\varphi(P)\right)^{\frac{1}{k}}\le R_1$. Similarly, we can get $\|Z(\cdot,t)\|_k\le\left(\int_\Omega Z^k\varphi(H)\right)^{\frac{1}{k}}\le R_2$, then we choose a constant R such that $R=\min\{R_1,R_2\}$, we can obviously get (2.13) which are the desired results.

Next we derive the L^∞-bound for $Z(x,t)$ by utilizing Lemma 2.5.

Lemma 2.6. *Let (P,H,Z) be a solution of the system (1.2). Assume that coefficients of (1.2) are always positive, then there exists a positive constant M such that $||Z(\cdot,t)||_\infty\le M$, for all $t\in(0,T_{\max})$.*

Proof. We employ semigroup arguments in [51] in order to attain the L^∞-bound of Z. As pointed in Lemma 2.5, through applying the variation of constants formula, we have

$$\begin{aligned} Z(\cdot,t) &= \mathrm{e}^{-t(A_{D_3}+1)}Z_0 - \chi_1\int_0^t \mathrm{e}^{-(t-s)(A_{D_3}+1)}\nabla\cdot(Z(\cdot,t))\nabla P(\cdot,t))\mathrm{d}s \\ &\quad + \chi_2\int_0^t \mathrm{e}^{-(t-s)(A_{D_3}+1)}\nabla\cdot(Z(\cdot,t))\nabla H(\cdot,t))\mathrm{d}s + \int_0^t \mathrm{e}^{-(t-s)(A_{D_3}+1)}F^{(3)}(P,H,Z)\mathrm{d}s \\ &:= E_1+E_2+E_3+E_4. \end{aligned}$$

Next, we proceed to prove the L^∞-bound for E_1, E_2, E_3 and E_4 separately. As in Lemma 2.5, we likewise select $\tau < 1$.

For E_1, we find that

$$||E_1(\cdot,t)||_\infty \le C_6\tau^{\vartheta}\mathrm{e}^{-\epsilon t}||Z_0||_q \le ||Z_0||_\infty, \text{ for all } t\in(\tau,T_{\max}), \tag{2.34}$$

where $\vartheta\in(\frac{n}{2q},1)$, $q=n+2$ and $\epsilon>0$.

For E_2, set $k=0$, $q=n+2$ and $p=\infty$ in Lemma 2.3, so we can choose $\theta\in\left(\frac{n}{2q},\frac{1}{2}\right)$. In this case, we have $\varepsilon\in(0,\frac{1}{2}-\theta)$. Then there exist positive constants C_7 and μ such that

$$\begin{aligned} ||E_2(\cdot,t)||_\infty &\le C_7||(A_{D_3}+1)^\theta E_2(\cdot,t)||_q = \chi_1 C_7\int_0^t ||(A_{D_3}+1)^\theta \mathrm{e}^{-(t-s)(A_{D_3}+1)}\nabla\cdot(Z(\cdot,t))\nabla P(\cdot,t))||_q\mathrm{d}s \\ &\le \chi_1 C_7\int_0^t \mathrm{e}^{-(t-s)}||(A_{D_3}+1)^\theta \mathrm{e}^{-(t-s)A_{D_3}}\nabla\cdot(Z(\cdot,t))\nabla P(\cdot,t))||_q\mathrm{d}s \\ &\le C_8\int_0^t (t-s)^{-\theta-\frac{1}{2}-\varepsilon}\mathrm{e}^{-(\mu+1)(t-s)}||Z(\cdot,t))\nabla P(\cdot,t)||_q\mathrm{d}s, \end{aligned}$$

for all $t\in(0,T_{\max})$.

From the previous analysis, it follows that for all $t\in(\tau,T_{\max})$, we can obtain $||\nabla P(\cdot,t)||_\infty \le G_1(\tau)$. This immediately yields the existence of a positive constant $C_9>0$ satisfying $||Z(\cdot,t))\nabla P(\cdot,t)||_q \le C_9$ over the same time interval.

Consequently, for all $t\in(\tau,T_{\max})$, we have

$$||E_2(\cdot,t)||_\infty \le C_8C_9\int(t-s)^{-\theta-\frac{1}{2}-\varepsilon}\mathrm{e}^{-(\mu+1)(t-s)}\mathrm{d}s \le C_8C_9\int_0^\infty \sigma^{-\theta-\frac{1}{2}-\tau}\mathrm{e}^{-(\mu+1)\sigma}\mathrm{d}\sigma \le C_{10}\Gamma(\zeta), \tag{2.35}$$

where $\Gamma(x)$ is the Gamma function. Given that $\zeta=\frac{1}{2}-\theta-\varepsilon>0$, then $\Gamma(\zeta)$ is real-valued and positive.

For E_3, applying the same way for E_2, we get that for all $t\in(\tau,T_{\max})$,

$$||E_3(\cdot,t)||_\infty \le C_{11}C_{12}\int(t-s)^{-\theta-\frac{1}{2}-\varepsilon}\mathrm{e}^{-(\mu+1)(t-s)}\mathrm{d}s \le C_{11}C_{12}\int_0^\infty \sigma^{-\theta-\frac{1}{2}-\tau}\mathrm{e}^{-(\mu+1)\sigma}\mathrm{d}\sigma \le C_{13}\Gamma(\zeta), \tag{2.36}$$

where $\Gamma(\zeta)$ is also real-valued and positive.

Ultimately, turning to E_4, the previously established (2.8) and (2.9) collectively give that for all $t \in (\tau, T_{\max})$,

$$\begin{aligned}||E_4(\cdot,t)||_{1,p} \leq & C_{15}||(A_{D_3}+1)^{\theta}E_4(\cdot,t)||_q \leq C_{14}\int_0^t (t-s)^{-\theta}\mathrm{e}^{-\gamma(t-s)}||F^{(3)}||_q \mathrm{d}s\\ \leq & C_{14}\int_0^t (t-s)^{-\theta}\mathrm{e}^{-\gamma(t-s)}\left(||P(\cdot,t)||_q + ||H(\cdot,t)+||Z(\cdot,t)||_q\right)\mathrm{d}s\\ \leq & C_{14}\int_0^t (t-s)^{-\theta}\mathrm{e}^{-\gamma(t-s)}\mathrm{d}s \leq C_{14}\int_0^{\infty}\sigma^{-\theta}\mathrm{e}^{-\gamma\sigma}\mathrm{d}\sigma\\ \leq & C_{14}\Gamma(1-\theta),\end{aligned}$$

where C_{14} represents a universal constant (possibly differing across derivations), and $\Gamma(1-\theta) > 0$ for $1-\theta > 0$.

For $p > n$, by the Sobolev embedding theorem, we have

$$||E_4(\cdot,t)||_{\infty} \leq C_{14}\Gamma(1-\theta) \text{ for all } t \in (\tau, T_{\max}). \tag{2.37}$$

Therefore, from (2.34), (2.35), (2.36) and (2.37), we conclude that $\|Z(\cdot,t)\|_{\infty}$ is bounded for $t \in (0, T_{\max})$. Coupled with Lemma 2.1, this establishes that $T_{\max} = \infty$ and therefore $(P(x,t), H(x,t), Z(x,t))$ is bounded for all $(x,t) \in \Omega \times (0,\infty)$.

Theorem 2.7. *Let Ω be a bounded domain in R^n $(n \geq 1)$ with smooth boundary $\partial\Omega$. Suppose that D_1, D_2, $D_3 > 0$, χ_1, χ_2 satisfies (2.12). For any $(P_0, H_0, Z_0) \in [W^{1,p}(\Omega)]^3$, where $p > n$, satisfying $P_0(x) \geq 0$, $H_0(x) \geq 0$, $Z_0(x) \geq 0$ for $x \in \Omega$, the system (1.2) possesses a unique global classical solution $(P(x,t), H(x,t), Z(x,t)) \in (C([0,\infty); W^{1,p}(\Omega)) \cap C^{2,1}(\overline{\Omega} \times (0,\infty)))^3$, which is bounded in $\Omega\times$ $(0,\infty)$, i.e. there is a constant $M(P_0, H_0, Z_0) > 0$ such that $||P(\cdot,t)||_{\infty} + ||H(\cdot,t)||_{\infty} + ||Z(\cdot,t)||_{\infty} \leq M(P_0, H_0, Z_0)$ for all $t \in [0,\infty)$.*

Proof. By synthesizing the conclusions from Lemma 2.1 with Lemma 2.6, the assertion of Theorem 2.7 is rigorously established.

3. Dynamics of the model on a Circular Domain

3.1. The existence of equilibria

First, we obtain the existence of equilibria. The boundary equilibrium points have been analyzed in detail in [34]. Here, we will not elaborate on them but will instead focus our analysis on the internal equilibrium point.

For the positive equilibrium $E^*(P^*, H^*, Z^*)$, P^*, H^* and Z^* satisfy the following equations if it exists,

$$\begin{cases} r_1\left(1-\dfrac{P}{K_1}\right) - a_1 H - \dfrac{b_1 Z}{c_1 + P + a\beta A} = 0,\\ r_2\left(1-\dfrac{H}{K_2}\right) - a_2 P - \dfrac{b_2 Z}{c_2 + \theta_1 P + \theta_2 H^2} = 0,\\ \dfrac{Z}{\delta + Z}\left(\dfrac{e_1(P+\beta A)}{c_1 + P + \alpha\beta A} - \dfrac{e_2 H}{c_2 + \theta_1 P + \theta_2 H^2}\right) - d_1 - d_2 Z = 0. \end{cases} \tag{3.1}$$

Following conventional approaches, one would attempt to directly solve the nonlinear system of equations (3.1) by expressing Z in terms of P and H, subsequently substituting these expressions into the third equation to establish the existence of solutions. However, the inherent complexity of (3.1) prevents the derivation of explicit analytical expressions through direct computation. Consequently, we prove the existence of solutions to the problem by constructing a compact convex set and applying the Brouwer fixed-point theorem.

Theorem 3.1. *Consider the nonlinear system (3.1), assume the following conditions hold,*

(H1). $a_1K_2 + \dfrac{b_1Z_{max}}{c_1 + a\beta A} \leq r_1,\ a_2K_1 + \dfrac{b_2Z_{max}}{c_2 + \theta_1K_1 + \theta_2K_2^2} \leq r_2,$
where $Z_{\max}$ *is defined as a value satisfying*

$$Z_{max} = \frac{1}{d_2}\left(\frac{e_1(K_1 + \beta A)}{c_1 + K_1 + a\beta A} - d_1\right).$$

(H2). *There exists* $P \in [0, K_1]$ *and* $H \in [0, K_2]$ *such that*

$$\frac{e_1(P + \beta A)}{c_1 + P + a\beta A} > \frac{e_2H}{c_2 + \theta_1P + \theta_2H^2}.$$

Then, the system admits at least one non-negative solution

$$(P^*, H^*, Z^*) \in D = [0, K_1] \times [0, K_2] \times [0, Z_{max}].$$

Proof.

As established in the preceding section, the variables P, H and Z are bounded. From the first two equations, it is straightforward to derive that the upper bounds for P and H are K_1 and K_2, respectively. Thus, $P \in [0, K_1]$ and $H \in [0, K_2]$.

For Z, analyze the asymptotic behavior of the third equation, as $Z \to \infty$, the equation approximates

$$\left(\frac{e_1(P + \beta A)}{c_1 + P + a\beta A} - \frac{e_2H}{c_2 + \theta_1P + \theta_2H^2}\right) - d_2Z \approx 0,$$

since $d_2 > 0$, the left-hand side becomes negative for sufficiently large Z. Hence, there exists $Z_{\max} > 0$ such that $Z \in [0, Z_{\max}]$.

Next, we proceed to construct a compact convex set. We define the domain

$$D = [0, K_1] \times [0, K_2] \times [0, Z_{\max}],$$

where $Z_{\max}$ satisfies $Z_{\max} \geq \dfrac{1}{d_2}\left(\dfrac{e_1(K_1 + \beta A)}{c_1 + K_1 + a\beta A} - d_1\right)$. Here, we choose $Z_{\max} = \dfrac{1}{d_2}\left(\dfrac{e_1(K_1 + \beta A)}{c_1 + K_1 + a\beta A} - d_1\right)$.

This domain D is closed, convex, and we define a continuous mapping $T : D \to D$ as

$$T(P, H, Z) = (P', H', Z'),$$

where P', H', Z' are solutions to the three equations, respectively.

Then we proceed to establish the continuity and self-mapping property of the operator$T$.

First, all denominators $c_1 + P + a\beta A$, $c_2 + \theta_1P + \theta_2H^2$, and $\delta + Z$ remain positive within D. Thus, the right-hand sides of the equations are continuous in P, H, Z, ensuring T is continuous.

And from the established boundedness of the variables, we can rigorously conclude that $P' \leq K_1$ and $H' \leq K_2$. In fact, to solve for P' from the first equation, it is essential to ensure $P' \leq K_1$. When $H = K_2$ and $Z = Z_{\max}$, the equation reduces to

$$r_1\left(1 - \frac{P'}{K_1}\right) = a_1K_2 + \frac{b_1Z_{\max}}{c_1 + P' + a\beta A},$$

when $P' = 0$, the right-hand side attains its maximum value

$$a_1K_2 + \frac{b_1Z_{\max}}{c_1 + a\beta A}.$$

At this point, the left-hand side equals r_1, therefore, the following inequality must hold to guarantee the existence of a solution

$$a_1 K_2 + \frac{b_1 Z_{\max}}{c_1 + a\beta A} \leq r_1,$$

while maintaining $P' \geq 0$, and $P' \leq K_1$.

Using the same method to discuss H, we can conclude that H needs to satisfy the condition

$$a_2 K_1 + \frac{b_2 Z_{\max}}{c_2 + \theta_1 K_1 + \theta_2 K_2^2} \leq r_2.$$

For Z, when $Z = Z_{\max}$, the left-hand side of the third equation is negative, forcing $Z' \leq Z_{\max}$. Therefore, the self-mapping property is satisfied.

Last, by applying the Brouwer Fixed-Point Theorem (Any continuous mapping from a compact convex set to itself has at least one fixed point.), we can obtain the following conclusion. Since $T : D \to D$ is continuous and D is compact and convex, there exists $(P^*, H^*, Z^*) \in D$ such that $T(P^*, H^*, Z^*) = (P^*, H^*, Z^*)$, proving the existence of a solution.

Furthermore, from a practical perspective grounded in biological relevance, it is imperative to establish the existence of positive equilibrium. Start with the third equation, when $Z > 0$, the equation can be arranged as

$$\frac{Z}{\delta + Z} \cdot W = d_1 + d_2 Z, \tag{3.2}$$

where

$$W = \frac{e_1(P + \beta A)}{c_1 + P + a\beta A} - \frac{e_2 H}{c_2 + \theta_1 P + \theta_2 H^2}.$$

Since the right-hand side of (3.2) is strictly positive, it follows that $W > 0$, thereby establishing condition (H2).

3.2. The existence of the Hopf bifurcation

This section investigates the equilibrium of system (1.2) using linear stability methods, with particular emphasis on characterizing both standard and equivariant Hopf bifurcations near E^*.

To ascertain the local stability of the equilibrium $E^*(P^*, H^*, Z^*)$, we need to calculate the linearized system of (1.2) at E^*. In fact, letting $X = (P, H, Z)^{\mathrm{T}}$, $X_\tau = (P_\tau, H_\tau, Z_\tau)^{\mathrm{T}}$, the linearized system of (1.2) around (P^*, H^*, Z^*) is

$$\frac{\partial X}{\partial t} = D\Delta X + AX + BX_\tau,$$

where

$$D = \begin{pmatrix} D_1 & 0 & 0 \\ 0 & D_2 & 0 \\ -\chi_1 Z^* & \chi_2 Z^* & D_3 \end{pmatrix}, \quad A = \begin{pmatrix} -a_{11} & -a_{12} & -a_{13} \\ -a_{21} & -a_{22} & -a_{23} \\ 0 & 0 & -a_{33} \end{pmatrix}, \quad B = \begin{pmatrix} 0 & 0 & 0 \\ 0 & 0 & 0 \\ -a_{31} & -a_{32} & 0 \end{pmatrix},$$

with

$$a_{11}=\frac{r_1P^*}{K_1}-\frac{b_1P^*Z^*}{(c_1+P^*+\alpha\beta A)^2},\quad a_{12}=a_1P^*,\quad a_{13}=\frac{b_1P^*}{c_1+P^*+\alpha\beta A},\quad a_{21}=a_2H^*-\frac{b_2\theta_1H^*Z^*}{(c_2+\theta_1P^*+\theta_2H^{*2})^2},$$
$$a_{22}=\frac{r_2H^*}{K_2}-\frac{2b_2\theta_2H^{*2}Z^*}{(c_2+\theta_1P^*+\theta_2H^{*2})^2},\quad a_{23}=\frac{b_2H^*}{c_2+\theta_1P^*+\theta_2H^{*2}},\quad a_{32}=\frac{e_2Z^{*2}}{(\delta+Z^*)}\left(\frac{c_2+\theta_1P^*-\theta_2H^{*2}}{(c_2+\theta_1P^*+\theta_2H^{*2})^2}\right),$$
$$a_{31}=-\frac{Z^{*2}}{\delta+Z^*}\left(\frac{e_1c_1+e_1\alpha\beta A-e_1\beta A}{(c_1+P^*+\alpha\beta A)^2}+\frac{e_2\theta_1H^*}{(c_2+\theta_1P^*+\theta_2H^{*2})^2}\right),\quad a_{33}=-\frac{\delta d_1}{\delta+Z^*}+\frac{d_2*Z^{*2}}{\delta+Z^*}. \tag{3.3}$$

On a disk, the characteristic equation of the linearized system restricted to span $\left\{\hat{\phi}^c_{0p},\hat{\phi}^c_{nm},\hat{\phi}^s_{nm}\right\}$ has the following form,

$$\prod_p\Delta_{0p}(\gamma)\prod_{n,m}\Delta_{nm}(\gamma)=0,$$

with

$$\Delta_{0p}(\gamma)=\det\left[\gamma I+\lambda_{0p}D-A-B(\mathrm{e}^{\gamma\cdot}I)\right]=0,\ p=0,1,2,\cdots, \tag{3.4}$$

$$\Delta_{nm}(\gamma)=\det\left[\gamma I+\lambda_{nm}D-A-B(\mathrm{e}^{\gamma\cdot}I)\right]^2=0,\ n,\ m=1,2,\cdots, \tag{3.5}$$

where

$$\lambda_{0p}=\frac{\alpha^2_{0p}}{R^2},\ p=0,1,2,\cdots,\ \lambda_{nm}=\frac{\alpha^2_{nm}}{R^2},\ n=1,2,\cdots,\ m=1,2,\cdots,$$
$$\hat{\phi}^c_{0p}=\frac{\phi^c_{0p}}{\|\phi^c_{0p}\|_{2,2}},\quad \hat{\phi}^c_{nm}=\frac{\phi^c_{nm}}{\|\phi^c_{nm}\|_{2,2}},\quad \hat{\phi}^s_{nm}=\frac{\phi^s_{nm}}{\|\phi^s_{nm}\|_{2,2}},$$
$$\phi^c_{0p}=J_0\left(\frac{\alpha_{0p}}{R}r\right),\quad \phi^c_{nm}=J_n\left(\frac{\alpha_{nm}}{R}r\right)\mathrm{e}^{\mathrm{i}n\theta},\quad \phi^s_{nm}=J_n\left(\frac{\alpha_{nm}}{R}r\right)\mathrm{e}^{-\mathrm{i}n\theta}.$$

Besides, α_{0p} and α_{nm} are eigenvalues of the Laplacian on the unit disk with homogeneous Neumann boundary condition [41]. And J_n $(n=0,1,\cdots)$ denotes the Bessel function of the first kind, with the explicit form $J_n(\rho)=\sum_{m=0}^{+\infty}\frac{(-1)^m}{m!\,\Gamma(n+m+1)}\left(\frac{\rho}{2}\right)^{n+2m}$. What's more, if the equation (3.4) has a pair of conjugate pure virtual roots and satisfies the transversal condition, then the central subspace of the equilibrium point is two-dimensional, then the original system is said to generate Hopf bifurcation at this point. If the equation (3.5) has a pair of conjugate pure imaginary roots and satisfies the transversal condition, then the pure imaginary root is a double root of the characteristic equation, and the central subspace of the equilibrium point is four-dimensional, then the original system generates an equivariant Hopf bifurcation at this point. Since the analysis method is the same, we only analyze the second equation concretely to avoid repetition.

The expression of the characteristic equation of (3.5) can be obtained by direct calculation in the following form,

$$\Delta_{nm}=\gamma^3+C_{1nm}\gamma^2+C_{2nm}\gamma+C_{3nm}+(C_{4nm}\gamma+C_{5nm})\,\mathrm{e}^{-\gamma\tau}=0, \tag{3.6}$$

where
$C_{1nm}=a_{11}+a_{22}+a_{33}+(D_1+D_2+D_3)\lambda_{nm}$,
$C_{2nm}=(D_1D_2+D_1D_3+D_2D_3)\lambda^2_{nm}+[(a_{22}+a_{33})D_1+(a_{11}+a_{33})D_2+(a_{22}+a_{11})D_3+(a_{13}\chi_1-a_{23}\chi_2)Z^*]\,\lambda_{nm}+a_{11}a_{22}+a_{11}a_{33}+a_{22}a_{33}-a_{12}a_{21}$,

$C_{3nm} = D_1D_2D_3\lambda_{nm}^3 + (a_{33}D_1D_2 + a_{22}D_1D_3 + a_{11}D_2D_3 + Z^*a_{13}\chi_1D_2 - Z^*a_{23}\chi_2D_1)\lambda_{nm}^2 + (a_{22}a_{33}D_1 + a_{11}a_{33}D_2 + a_{22}a_{11}D_3 - a_{12}a_{21}D_3 + Z^*a_{13}a_{22}\chi_1 - Z^*a_{21}a_{23}\chi_1 + Z^*a_{13}a_{21}\chi_2 - Z^*a_{11}a_{23}\chi_2)\lambda_{nm} + a_{11}a_{22}a_{33} - a_{12}a_{21}a_{33}$,
$C_{4nm} = -(a_{13}a_{31} + a_{23}a_{32})$,
$C_{5nm} = -(a_{23}a_{32}D_1 + a_{13}a_{31}D_2)\lambda_{nm} - a_{13}a_{22}a_{31} + a_{12}a_{23}a_{31} + a_{13}a_{21}a_{32} - a_{11}a_{23}a_{32}$.

We omit the subscript nm for simplicity. And the Routh-Hurwitz criterion leads to the following lemma.

Lemma 3.2. *All roots of the equation (3.6) have negative real part if and only if* $C_1 > 0,\ C_1(C_2 + C_4) - (C_3 + C_5) > 0,\ C_3 + C_5 > 0.$

Then we know that the positive equilibrium point E^* is asymptotically stable when $\tau = 0$.

Next consider the case of $\tau > 0$. Let $\lambda = \mathrm{i}\omega$ $(\omega > 0)$ is the root of (3.6), then ω satisfy

$$-\mathrm{i}\omega^3 - C_1\omega^2 + C_2\mathrm{i}\omega + C_3 + (C_4\mathrm{i}\omega + C_5)\,\mathrm{e}^{-\mathrm{i}\omega\tau} = 0,$$

then obtained by separating the real and imaginary parts that

$$\begin{cases} C_1\omega^2 - C_3 = C_4\omega\sin\omega\tau + C_5\cos\omega\tau, \\ -\omega^3 + C_2\omega = -C_4\omega\cos\omega\tau + C_5\sin\omega\tau. \end{cases}$$

Square and add the above two equations,

$$\omega^6 + (C_1^2 - 2C_2)\omega^4 + (C_2^2 - 2C_1C_3 - C_4^2)\omega^2 + C_3^2 - C_5^2 = 0.$$

Let $z = \omega^2$, then

$$z^3 + (C_1^2 - 2C_2)z^2 + (C_2^2 - 2C_1C_3 - C_4^2)z + C_3^2 - C_5^2 = 0.$$

Define

$$g_{nm}(z) = z^3 + (C_1^2 - 2C_2)z^2 + (C_2^2 - 2C_1C_3 - C_4^2)z + C_3^2 - C_5^2 := z^3 + R_{nm}z^2 + N_{nm}z + H_{nm}.$$

Lemma 3.3.

(1) When $H_{nm} < 0$ *holds,* $g_{nm}(z) = 0$ *has at least one positive real root;*

(2) when $H_{nm} \geq 0, R_{nm}^2 - -3N_{nm} > 0$ *hold,* $g_{nm}(z) = 0$ *has positive real roots if and only if* $\alpha_{nm}^+ > 0, g_{nm}(\alpha_{nm}^+) \leq 0$;

(3) when $H_{nm} \geq 0, R_{nm}^2 - 3N_{nm} \leq 0$ *hold,* $g_{nm}(z) = 0$ *has no positive real roots;*

where $\alpha_{nm}^+ = \dfrac{-R_{nm} + \sqrt{R_{nm}^2 - 3H_{nm}}}{3}$.

Proof.

For (1), evidently, $g_{nm}(0) = H_{nm}$, $\lim\limits_{z\to+\infty} g_{nm}(z) = +\infty$, so when $H_{nm} < 0$ holds, $g_{nm}(z) = 0$ has at least one positive real root.

For (2), taking the derivative of $g_{nm}(z)$, we can get that $g'_{nm}(z) = 3z^2 + 2R_{nm}z + N_{nm}$, when the discriminant $R_{nm}^2 - 3N_{nm} > 0,\ H_{nm} \geq 0,\ g'_{nm}(z)$ has two real roots,

$$\alpha_{nm}^+ = \frac{-R_{nm} + \sqrt{R_{nm}^2 - 3N_{nm}}}{3},\ \alpha_{nm}^- = \frac{-R_{nm} - \sqrt{R_{nm}^2 - 3N_{nm}}}{3}.$$

Obviously,

$$g''_{nm}(\alpha^+_{nm}) = 2\sqrt{R^2_{nm} - 3N_{nm}} > 0, \quad g''_{nm}(\alpha^-_{nm}) = -2\sqrt{R^2_{nm} - 3N_{nm}} < 0.$$

Hence, α^+_{nm} is the local minimum point of $g_{nm}(z)$, α^-_{nm} is the local maximum point of $g_{nm}(z)$. The sufficiency is clearly established, for the necessity, assume that $\alpha^+_{nm} \le 0$ or $\alpha^+_{nm} > 0,\ g_{nm}(\alpha^+_{nm}) > 0$ hold, when $z \ge \alpha^+_{nm}$, $g_{nm}(z)$ is an increasing function and $g_{nm}(0) \ge 0$, therefore, the condition $\alpha^+_{nm} \le 0$ is satisfied, $g_{nm}(z)$ has no positive real roots. α^-_{nm} is the local maximum point of $g_{nm}(z)$, so $g_{nm}(\alpha^+_{nm}) < g_{nm}(\alpha^-_{nm})$. Hence when $\alpha^+_{nm} > 0,\ g_{nm}(\alpha^+_{nm}) > 0,\ H_{nm} \ge 0$ hold, $g_{nm}(z)$ has no positive real roots.

For (3), when $R^2_{nm} - 3N_{nm} \le 0,\ z \in [0, +\infty),\ g_{nm}(z)$ is a monotone non-decreasing function. At this point, if $H_{nm} \ge 0$, then $g_{nm}(z)$ has no positive real roots.

Define that $G = \{(n, m) \in (\mathbb{N}^*, \mathbb{N}^*);\ H_{nm} < 0 \,\text{or}\, H_{nm} \ge 0,\ \alpha^+_{nm} > 0,\ g_{nm}(\alpha^+_{nm}) \le 0,\ R^2_{nm} - 3N_{nm} > 0\}$, there is no harm in supposing that the three positive roots of $g_{nm}(z)$ are $z^{(1)}_{nm},\ z^{(2)}_{nm},\ z^{(3)}_{nm}$, then $\omega^{(i)}_{nmj} = (z^{(i)}_{nm})^{\frac{1}{2}},\ i = 1, 2, 3$.

Therefore, we can obtain

$$\cos \omega^{(i)}_{nmj}\tau^{(i)}_{nmj} = \frac{C_5\left(C_1\left(\omega^{(i)}_{nmj}\right)^2 - C_3\right) + C_4\omega^{(i)}_{nmj}\left(\left(\omega^{(i)}_{nmj}\right)^3 - C_2\omega^{(i)}_{nmj}\right)}{C_4^2\left(\omega^{(i)}_{nmj}\right)^2 + C_5^2},$$

so,

$$\tau^{(i)}_{nmj} = \begin{cases} \frac{1}{\omega^{(i)}_{nmj}}\left[\arccos \frac{C_5\left(C_1\left(\omega^{(i)}_{nmj}\right)^2 - C_3\right) + C_4\omega^{(i)}_{nmj}\left(\left(\omega^{(i)}_{nmj}\right)^3 - C_2\omega^{(i)}_{nmj}\right)}{C_4^2\left(\omega^{(i)}_{nmj}\right)^2 + C_5^2} + 2j\pi\right], & \sin \omega^{(i)}_{nmj}\tau^{(i)}_{nmj} \ge 0, \\ \frac{1}{\omega^{(i)}_{nmj}}\left[-\arccos \frac{C_5\left(C_1\left(\omega^{(i)}_{nmj}\right)^2 - C_3\right) + C_4\omega^{(i)}_{nmj}\left(\left(\omega^{(i)}_{nmj}\right)^3 - C_2\omega^{(i)}_{nmj}\right)}{C_4^2\left(\omega^{(i)}_{nmj}\right)^2 + C_5^2} + 2(j+1)\pi\right], & \sin \omega^{(i)}_{nmj}\tau^{(i)}_{nmj} < 0. \end{cases}$$

where $i = 1, 2, 3;\ j = 0, 1, 2, \cdots, m,\ n \in G$.

Define

$$\tau^* = \min_{i=1,2,3} \tau^{(i)}_{nm0}.$$

Assume that $\gamma_{nm}(\tau) = \alpha_{nm}(\tau) + \mathrm{i}\beta_{nm}(\tau)$ is the root of the equation (3.6) near $\tau = \tau^{(i)}_{nmj}$, and satisfy $\alpha_{nm}(\tau^{(i)}_{nmj}) = 0,\ \beta_{nm}(\tau^{(i)}_{nmj}) = \omega^{(i)}_{nmj},\ j = 0, 1, 2, \cdots$, then we have the following transversal conditions.

Lemma 3.4. *When* $g'_{nm}\left(\omega^{(i)}_{nmj}\right)^2 \ne 0,\ \alpha'_{nm}(\tau^{(i)}_{nmj}) \ne 0$ *holds.*

Proof. Take the derivative of τ on both sides of the equation (3.6),

$$\frac{\mathrm{d}\gamma}{\mathrm{d}\tau}\left(3\gamma^2 + 2C_1\gamma + C_2 + C_4\mathrm{e}^{-\gamma\tau} - \tau\left(C_4\gamma + C_5\right)\mathrm{e}^{-\gamma\tau}\right) = \gamma\left(C_4\gamma + C_5\right)\mathrm{e}^{-\gamma\tau},$$

so we have

$$\left(\frac{\mathrm{d}\gamma}{\mathrm{d}\tau}\right)^{-1} = \frac{\left(3\gamma^2 + 2C_1\gamma + C_2\right)\mathrm{e}^{\gamma\tau}}{\gamma(C_4\gamma + C_5)} + \frac{C_4}{(C_4\gamma + C_5)\gamma} - \frac{\tau}{\gamma},$$

then

$$\left[\frac{\mathrm{d}(\mathrm{Re}\gamma)}{\mathrm{d}\tau}\right]^{-1}\Big|_{\tau=\tau_{nmj}^{(i)}} = \mathrm{Re}\left[\frac{\mathrm{d}\lambda}{\mathrm{d}\tau}\right]^{-1}\Big|_{\tau=\tau_{nmj}^{(i)}} = \frac{3\left(\omega_{nmj}^{(i)}\right)^4 + (2C_1^2 - 4C_2)\left(\omega_{nmj}^{(i)}\right)^2 + C_2^2 - C_4^2 - 2C_1C_3}{C_4^2\left(\omega_{nmj}^{(i)}\right)^2 + C_5^2}$$
$$= \frac{g'_{nm}\left(\omega_{nmj}^{(i)}\right)^2}{C_4^2\left(\omega_{nmj}^{(i)}\right)^2 + C_5^2},$$

so, we have

$$\mathrm{sgn}\{\alpha'_{nm}(\tau_{nmj}^{(i)})\} = \mathrm{sgn}\left\{g'_{nm}\left(\omega_{nmj}^{(i)}\right)^2\right\}.$$

Therefore, when $g'_{nm}\left(\omega_{nmj}^{(i)}\right)^2 \neq 0$, $\alpha'_{nm}(\tau_{nmj}^{(i)}) \neq 0$.

Subsequently, we arrive at the theorem outlined below.

Theorem 3.5. *When the system (1.2) satisfies the conditions in Lemma 3.2.*

(1) If $H_{nm} \geq 0$, $R_{nm}^2 - 3N_{nm} \leq 0$, then the internal equilibrium point E^* of (1.2) is locally asymptotically stable for all $\tau > 0$.

(2) If $m \in G$, then there exists $\tau^* > 0$, when $\tau \in [0, \tau^*)$, the internal equilibrium E^* is locally asymptotically stable; when $\tau > \tau^*$, the internal equilibrium E^* is not stable.

(3) If $n,\ m \in G$, $g'_{nm}\left(\omega_{nmj}^{(i)}\right)^2 \neq 0$, then when $\tau = \tau_{nmj}^{(i)}$, $i = 1, 2, 3$, the system may undergo equivariant Hopf bifurcation near the internal equilibrium E^*.

Remark 3.6. Obviously, the conclusion of Theorem 3.5 is relatively rough, because the three roots of (3.6) do not necessarily exist at the same time, but because of the complexity of the cubic equation, it is difficult to give the condition of the existence of a specific number of roots. Here we focus on the analysis of the specific situation of equivariant Hopf bifurcations when two roots exist at the same time, because this time will result in the stable switch. Now we give the following theorem.

Theorem 3.7. *The hypothesis in Theorem 3.5 are still true. And suppose that the delay values corresponding to the two roots are respectively τ_{11j}^+ and τ_{11j}^- when choosing $n = 1,\ m = 1$.*

(1) $\mathrm{Re}\left(\frac{\mathrm{d}\gamma}{\mathrm{d}\tau}\right)|_{\tau=\tau_{11j}^+} > 0$, $\mathrm{Re}\left(\frac{\mathrm{d}\gamma}{\mathrm{d}\tau}\right)|_{\tau=\tau_{11j}^-} < 0$.

(2) If $\tau_{1,1,0}^- > \tau_{1,1,1}^+$, the equilibrium E^* is locally asymptotically stable when $\tau \in [0, \tau_{1,1,0}^+)$; is unstable when $\tau \in (\tau_{1,1,0}^+, +\infty)$, and a family of nonhomogeneous periodic solution bifurcations is generated nearby $\tau = \tau_{11j}^{\pm}$, $j = 0, 1, 2, \cdots$.

(3) If $\tau_{1,1,0}^- < \tau_{1,1,1}^+$, there is a positive integer k, so that the equilibrium point E goes through k times from stable to unstable, then from unstable to stable, and finally to be unstable, that is to say, E is asymptotically stable when

$$\tau \in [0, \tau_{1,1,0}^+) \cup (\tau_{1,1,0}^-, \tau_{1,1,1}^+) \cup \cdots \cup (\tau_{1,1,k-1}^-, \tau_{1,1,k}^+),$$

and is unstable when

$$\tau \in (\tau_{1,1,0}^+, \tau_{1,1,0}^-) \cup (\tau_{1,1,1}^+, \tau_{1,1,1}^-) \cup \cdots \cup (\tau_{1,1,k-1}^+, \tau_{1,1,k-1}^-) \cup (\tau_{1,1,k}^+, +\infty),$$

additionally, $\tau = \tau_{11j}^{\pm}\ (j = 0, 1, 2, \cdots)$ *is a series of equivariant Hopf bifurcation values of the system, and these bifurcation periodic solutions are spatially inhomogeneous.*

Remark 3.8. It is worth noting that in Theorem 3.7, we only give the case of $m = 1,\ n = 1$, in fact, as long as $m,\ n \in G$ and satisfies the conditions under which bifurcations occur, there are similar theorems.

Remark 3.9. For (3.4), similar to the above analysis, we can also obtain conditions for the generation of Hopf bifurcation, which is the following theorem.

Theorem 3.10. *The system* (1.2) *has the positive equilibrium point* E^* *and satisfies the conditions in lemma 3.2. Define that* $\hat{G} = \{p \in \mathbb{N};\ H_{0p} < 0$ *or* $H_{0p} \geq 0,\ \alpha_{0p}^{+} > 0,\ g_{0p}(\alpha_{0p}^{+}) \leq 0,\ R_{0p}^2 - 3N_{0p} > 0\}$, *if* $p \in \hat{G}$, $g_{0p}'\left(\omega_{0pj}^{(i)}\right)^2 \neq 0$, *then when* $\tau = \tau_{0pj}^{(i)},\ i = 1, 2, 3$, *the system may undergo Hopf bifurcation near the internal equilibrium* E^*.

3.3. The normal form

Now we proceed to derive the reduced dynamics of system (1.2) in the neighborhood of the non-trivial equilibrium $E^*(P^*, H^*, Z^*)$ with regarding time delay τ as the key parameter for center manifold reduction.

Letting $\bar{P}(r, \theta, t) = P(r, \theta, \tau t) - P^*, \bar{H}(r, \theta, t) = H(r, \theta, \tau t) - H^*, \bar{Z}(r, \theta, t) = Z(r, \theta, \tau t) - Z^*$, we simplify the expression by dropping the bar. Ulteriorly, write $P(r, \theta, t)$ simply as P (H and Z is similar). With these notations, system (1.2) can be transformed into

$$\begin{cases} \dfrac{\partial P}{\partial t} = \tau D_1 \Delta_{r\theta} P + \tau[a_{11}(P + P^*) + a_{12}(H + H^*) + a_{13}(Z + Z^*)] + \tau \displaystyle\sum_{i+j+k\geq 2} F_{ijk}^{(1)}(0,0,0) P^i H^j Z^k, \\ \dfrac{\partial H}{\partial t} = \tau D_2 \Delta_{r\theta} H + \tau[a_{21}(P + P^*) + a_{22}(H + H^*) + a_{23}(Z + Z^*)] + \tau \displaystyle\sum_{i+j+k\geq 2} F_{ijk}^{(2)}(0,0,0) P^i H^j Z^k, \\ \dfrac{\partial Z}{\partial t} = \tau D_3 \Delta_{r\theta} Z - \tau \nabla_{r\theta} \cdot (\chi_1 Z \nabla_{r\theta} P) + \tau \nabla_{r\theta} \cdot (\chi_2 Z \nabla_{r\theta} H) + \tau[a_{33}(Z + Z^*)] \\ \qquad + \tau[a_{31}(P(r, \theta, t-1) + P^*) + a_{32}(H(r, \theta, t-1) + H^*)] \\ \qquad + \tau \displaystyle\sum_{i+j+k\geq 2} F_{ijk}^{(3)}(0,0,0) P^i(r, \theta, t-1) H^j(r, \theta, t-1) Z^k. \end{cases}$$

For simplicity, write it down as follows,

$$\begin{cases} \dfrac{\partial P}{\partial t} = \tau D_1 \Delta_{r\theta} P + \tau[a_{11}(P + P^*) + a_{12}(H + H^*) + a_{13}(Z + Z^*)] + F^{(4)}(P, H, Z), \\ \dfrac{\partial H}{\partial t} = \tau D_2 \Delta_{r\theta} H + \tau[a_{21}(P + P^*) + a_{22}(H + H^*) + a_{23}(Z + Z^*)] + F^{(5)}(P, H, Z), \\ \dfrac{\partial Z}{\partial t} = \tau D_3 \Delta_{r\theta} Z - \tau \nabla_{r\theta} \cdot (\chi_1 Z \nabla_{r\theta} P) + \tau \nabla_{r\theta} \cdot (\chi_2 Z \nabla_{r\theta} H) + \tau[a_{33}(Z + Z^*)] \\ \qquad + \tau[a_{31}(P(r, \theta, t-1) + P^*) + a_{32}(H(r, \theta, t-1) + H^*)] + F^{(6)}(P_\tau, H_\tau, Z), \end{cases}$$

where the expression of $a_{ij},\ i, j = 1, 2, 3$ was given in (3.3), and

$$F_{ijk}^{(1)} = \frac{1}{i!j!k!} \frac{\partial^{i+j+k} F^{(1)}}{\partial p^i \partial H^j \partial Z^k}(0,0,0),\ F_{ijk}^{(2)} = \frac{1}{i!j!k!} \frac{\partial^{i+j+k} F^{(2)}}{\partial p^i \partial H^j \partial Z^k}(0,0,0),$$
$$F_{ijk}^{(3)} = \frac{1}{i!j!k!} \frac{\partial^{i+j+k} F^{(3)}}{\partial P^i(t-\tau) \partial H^j(t-\tau) \partial Z^k}(0,0,0).$$

Introducing the bifurcation parameterization $\tau = \tau^* + \mu$, where $\mu \in \mathbb{R}$ and τ^* is the critical value at which equivariant Hopf bifurcations emerge, we reformulate the system as

$$\frac{\partial X}{\partial t} = D(\tau)\Delta_{r\theta}X + L(\tau)X_t + F(X_t, \tau).$$

Introducing μ as the perturbation parameter, To proceed with the Taylor expansions of $L(\tau)$ and $D(\tau)$, we write them as

$$\begin{aligned} L(\tau) &= L(\tau^* + \mu) = \tilde{L}_0 + \mu\tilde{L}_1 + \frac{1}{2}\mu^2\tilde{L}_2 + \cdots, \\ D(\tau) &= D(\tau^* + \mu) = \tilde{D}_0 + \mu\tilde{D}_1 + \frac{1}{2}\mu^2\tilde{D}_2 + \cdots, \end{aligned}$$

and here $\tilde{D}_0 = D(\tau^*)$, $\tilde{L}_0(\cdot) = L(\tau^*)(\cdot)$ is a linear operator from $\mathscr{C}$ to $\mathscr{X}_{\mathbb{C}}$, where $\mathscr{C} := C([-\tau, 0],\ \mathscr{X}_{\mathbb{C}})$, $\mathscr{X}_{\mathbb{C}} = \{X(r,\theta) \in W^{2,2}(\Omega) : \partial_r X(R,\theta) = 0,\ \theta \in [0, 2\pi)\}$. Now, in the space $\mathscr{C}$, the dynamical equations admit the following operator formalism

$$\frac{\mathrm{d}X(t)}{\mathrm{d}t} = \tilde{D}_0\Delta_{r\theta}X(t) + \tilde{L}_0X_t + \tilde{F}(X_t, \mu), \tag{3.7}$$

where the operators L_0 and $\tilde{F}$ are defined as follows,

$$L_0(\varphi) = (\tau^* + \mu)\begin{pmatrix} a_{11}\varphi_1(0) + a_{12}\varphi_2(0)a_{13}\varphi_3(0) \\ a_{21}\varphi_1(0) + a_{22}\varphi_2(0)a_{23}\varphi_3(0) \\ a_{31}\varphi_1(-1) + b_{32}\varphi_2(-1) + a_{33}\varphi_3(0) \end{pmatrix},$$

$$\tilde{F}(\varphi, \mu) = (\tau^* + \mu)\left(F^{(4)}(P, H, Z), F^{(5)}(P, H, Z), F^{(6)}(P_\tau, H_\tau, Z)\right)^{\mathrm{T}},$$

and

$$\tilde{D}_0 = D,\ X(t) = (P(t), H(t), Z(t))^{\mathrm{T}},\ \varphi = (\varphi_1, \varphi_2, \varphi_3)^{\mathrm{T}} \in \mathscr{C}.$$

The linearization system of (3.7) is obtained,

$$\frac{\mathrm{d}X(t)}{\mathrm{d}t} = \tilde{D}_0\Delta_{r\theta}X(t) + \tilde{L}_0X_t. \tag{3.8}$$

Consider the operator $A : \mathscr{C} \to \mathscr{X}_{\mathbb{C}}$, which represents the infinitesimal generators of the semigroup arising from the solutions of (3.8), with A^* denoting the adjoint operator of A, and they satisfy

$$A\varphi(\vartheta) = \begin{cases} \varphi'(\vartheta), & \vartheta \in [-1, 0), \\ \int_{-\tau}^{0} \mathrm{d}\eta(\mu, \vartheta)\varphi(\vartheta), & \vartheta = 0, \end{cases} \quad \text{and} \quad A^*\psi(\varrho) = \begin{cases} -\psi'(\varrho), & \varrho \in (0, 1], \\ \int_{-\tau}^{0} \psi(-\varrho)\mathrm{d}\eta(\mu, \vartheta), & \varrho = 0, \end{cases}$$

and define a bilinear pairing

$$(\psi, \varphi) = \int_0^R \int_0^{2\pi} r\left[\overline{\psi(0)}\varphi(0)\right] - \int_{-\tau}^{0}\int_{\xi=0}^{\vartheta} \overline{\psi(\xi - \vartheta)}\mathrm{d}\eta(\tau^*, \vartheta)\varphi(\xi)\mathrm{d}\xi\Big] \,\mathrm{d}r\mathrm{d}\theta. \tag{3.9}$$

Subsequently, we introduce P and P^* as the generalized eigenspace of A and A^* associated with the set $\Lambda_0 = \{\mathrm{i}\omega_{\hat{\lambda}}, -\mathrm{i}\omega_{\hat{\lambda}}, \mathrm{i}\omega_{\hat{\lambda}}, -\mathrm{i}\omega_{\hat{\lambda}}, \}$, where P^* denotes the dual space of P. Then we write $\mathscr{C} = P_{\mathrm{C}} \oplus Q$, where P_{C} represents the central subspace, besides, Q is its complementary space.

The bases of P and P^* has the following form,

$$\Phi_{r\theta}(\vartheta) = \left(\Phi^1_{r\theta}(\vartheta),\ \Phi^2_{r\theta}(\vartheta)\right), \quad \Psi_{r\theta}(\rho) = \left(\Psi^1_{r\theta}(\rho),\ \Psi^2_{r\theta}(\rho)\right)^{\mathrm{T}},$$

where

$$\begin{aligned}
\Phi^1_{r\theta}(\vartheta) &= \left(\Phi_1(\vartheta)\cdot\hat{\phi}^c_{nm},\ \Phi_2(\vartheta)\cdot\hat{\phi}^c_{nm}\right) = \left(\mathrm{e}^{\mathrm{i}\boldsymbol{\omega}_{\hat{\lambda}}\vartheta}\xi\hat{\phi}^c_{nm},\ \mathrm{e}^{-\mathrm{i}\boldsymbol{\omega}_{\hat{\lambda}}\vartheta}\bar{\xi}\hat{\phi}^c_{nm}\right),\\
\Phi^2_{r\theta}(\vartheta) &= \left(\Phi_3(\vartheta)\cdot\hat{\phi}^s_{nm},\ \Phi_4(\vartheta)\cdot\hat{\phi}^s_{nm}\right) = \left(\mathrm{e}^{\mathrm{i}\omega_{\hat{\lambda}}\vartheta}\xi\hat{\phi}^s_{nm},\ \mathrm{e}^{-\mathrm{i}\omega_{\hat{\lambda}}\vartheta}\bar{\xi}\hat{\phi}^s_{nm}\right),\\
\Psi^1_{r\theta}(\rho) &= \left(\Psi_1(\rho)\cdot\hat{\phi}^c_{nm},\ \Psi_2(\rho)\cdot\hat{\phi}^c_{nm}\right)^{\mathrm{T}} = \left(q^{-1}\mathrm{e}^{\mathrm{i}\omega_{\hat{\lambda}}\rho}\eta\hat{\phi}^c_{nm},\ \bar{q}^{-1}\mathrm{e}^{-\mathrm{i}\omega_{\hat{\lambda}}\rho}\bar{\eta}\hat{\phi}^c_{nm}\right)^{\mathrm{T}},\\
\Psi^2_{r\theta}(\rho) &= \left(\Psi_3(\rho)\cdot\hat{\phi}^s_{nm},\ \Psi_4(\rho)\cdot\hat{\phi}^s_{nm}\right)^{\mathrm{T}} = \left(q^{-1}\mathrm{e}^{\mathrm{i}\omega_{\hat{\lambda}}\rho}\eta\hat{\phi}^s_{nm},\ \bar{q}^{-1}\mathrm{e}^{-\mathrm{i}\omega_{\hat{\lambda}}\rho}\bar{\eta}\hat{\phi}^s_{nm}\right)^{\mathrm{T}}.
\end{aligned}$$

Choosing $\xi = (1, p_1, p_2)^{\mathrm{T}},\ \eta = (1, q_1, q_2)$ with

$$\begin{aligned}
p_1 &= \frac{a_{23}(\mathrm{i}\omega_{\hat{\lambda}} + D_1\lambda_{nm} - a_{11}) + a_{21}a_{13}}{a_{13}(\mathrm{i}\omega_{\hat{\lambda}} + D_2\lambda_{nm} - a_{22}) + a_{21}a_{23}},\quad p_2 = \frac{(\mathrm{i}\omega_{\hat{\lambda}} + D_1\lambda_{nm} - a_{11})(\mathrm{i}\omega_{\hat{\lambda}} + D_2\lambda_{nm} - a_{22}) - a_{21}^2}{a_{13}(\mathrm{i}\omega_{\hat{\lambda}} + D_2\lambda_{nm} - a_{22}) + a_{21}a_{23}},\\
q_1 &= \frac{-a_{21}(\mathrm{i}\omega_{\hat{\lambda}} + D_3\lambda_{nm} - a_{33}) - a_{13}(\mathrm{i}\omega_{\hat{\lambda}} + \chi_2 Z^*\lambda_{nm} - a_{32})}{a_{23}(\mathrm{i}\omega_{\hat{\lambda}} + \chi_2 Z^*\lambda_{nm} - a_{32}) + (\mathrm{i}\omega_{\hat{\lambda}} + D_2\lambda_{nm} - a_{22})(\mathrm{i}\omega_{\hat{\lambda}} + D_3\lambda_{nm} - a_{33})},\\
q_2 &= \frac{a_{13}(\mathrm{i}\omega_{\hat{\lambda}} + D_2\lambda_{nm} - a_{22}) - a_{21}a_{23}}{a_{23}(\mathrm{i}\omega_{\hat{\lambda}} + \chi_2 Z^*\lambda_{nm} - a_{32}) + (\mathrm{i}\omega_{\hat{\lambda}} + D_2\lambda_{nm} - a_{22})(\mathrm{i}\omega_{\hat{\lambda}} + D_3\lambda_{nm} - a_{33})},
\end{aligned}$$

then it follows that the bases of P is

$$\Phi_{r\theta}(\vartheta) = \begin{pmatrix}
\mathrm{e}^{\mathrm{i}\omega_{\hat{\lambda}}\tau^*\vartheta}\hat{\phi}^c_{nm} & \mathrm{e}^{-\mathrm{i}\omega_{\hat{\lambda}}\tau^*\vartheta}\hat{\phi}^c_{nm} & \mathrm{e}^{\mathrm{i}\omega_{\hat{\lambda}}\tau^*\vartheta}\hat{\phi}^s_{nm} & \mathrm{e}^{-\mathrm{i}\omega_{\hat{\lambda}}\tau^*\vartheta}\hat{\phi}^s_{nm}\\
p_1\mathrm{e}^{\mathrm{i}\omega_{\hat{\lambda}}\tau^*\vartheta}\hat{\phi}^c_{nm} & \bar{p}_1\mathrm{e}^{-\mathrm{i}\omega_{\hat{\lambda}}\tau^*\vartheta}\hat{\phi}^c_{nm} & p_1\mathrm{e}^{\mathrm{i}\omega_{\hat{\lambda}}\tau^*\vartheta}\hat{\phi}^s_{nm} & \bar{p}_1\mathrm{e}^{-\mathrm{i}\omega_{\hat{\lambda}}\tau^*\vartheta}\hat{\phi}^s_{nm}\\
p_2\mathrm{e}^{\mathrm{i}\omega_{\hat{\lambda}}\tau^*\vartheta}\hat{\phi}^c_{nm} & \bar{p}_2\mathrm{e}^{-\mathrm{i}\omega_{\hat{\lambda}}\tau^*\vartheta}\hat{\phi}^c_{nm} & p_2\mathrm{e}^{\mathrm{i}\omega_{\hat{\lambda}}\tau^*\vartheta}\hat{\phi}^s_{nm} & \bar{p}_2\mathrm{e}^{-\mathrm{i}\omega_{\hat{\lambda}}\tau^*\vartheta}\hat{\phi}^s_{nm}
\end{pmatrix},$$

and the basis of P^* is

$$\Psi_{r\rho}(\varrho) = \begin{pmatrix}
q^{-1}\mathrm{e}^{\mathrm{i}\omega_{\hat{\lambda}}\tau^*\varrho}\hat{\phi}^c_{nm} & \bar{q}^{-1}\mathrm{e}^{-\mathrm{i}\omega_{\hat{\lambda}}\tau^*\varrho}\hat{\phi}^c_{nm} & q^{-1}\mathrm{e}^{\mathrm{i}\omega_{\hat{\lambda}}\tau^*\varrho}\hat{\phi}^s_{nm} & \bar{q}^{-1}\mathrm{e}^{-\mathrm{i}\omega_{\hat{\lambda}}\tau^*\varrho}\hat{\phi}^s_{nm}\\
q_1q^{-1}\mathrm{e}^{\mathrm{i}\omega_{\hat{\lambda}}\tau^*\varrho}\hat{\phi}^c_{nm} & \bar{q}_1\bar{q}^{-1}\mathrm{e}^{-\mathrm{i}\omega_{\hat{\lambda}}\tau^*\varrho}\hat{\phi}^c_{nm} & q_1q^{-1}\mathrm{e}^{\mathrm{i}\omega_{\hat{\lambda}}\tau^*\varrho}\hat{\phi}^s_{nm} & \bar{q}_1\bar{q}^{-1}\mathrm{e}^{-\mathrm{i}\omega_{\hat{\lambda}}\tau^*\varrho}\hat{\phi}^s_{nm}\\
q_2q^{-1}\mathrm{e}^{\mathrm{i}\omega_{\hat{\lambda}}\tau^*\varrho}\hat{\phi}^c_{nm} & \bar{q}_2\bar{q}^{-1}\mathrm{e}^{-\mathrm{i}\omega_{\hat{\lambda}}\tau^*\varrho}\hat{\phi}^c_{nm} & q_2q^{-1}\mathrm{e}^{\mathrm{i}\omega_{\hat{\lambda}}\tau^*\varrho}\hat{\phi}^s_{nm} & \bar{q}_2\bar{q}^{-1}\mathrm{e}^{-\mathrm{i}\omega_{\hat{\lambda}}\tau^*\varrho}\hat{\phi}^s_{nm}
\end{pmatrix}^{\mathrm{T}},$$

where q can also be obtained by $(\Psi_{r\theta}, \Phi_{r\theta}) = I_4$, as per the adjoint bilinear operation specified by (3.9).

One can decompose X_t into two parts,

$$X_t = X_t^{P_C} + X_t^Q = \sum_{k=1}^{2}\Phi^k_{r\theta}(\Psi^k_{r\theta}, X_t) + X_t^Q = \sum_{k=1}^{2}\Phi^k_{r\theta}z^k_{r\theta} + y_t,$$

where $z^k_{r\theta} = (\Psi^k_{r\theta}, X_t),\ y_t \in Q$. Let the local coordinate system $z = (z_1, z_2, z_3, z_4)^{\mathrm{T}}$ parametrize the four-dimensional center manifold, where this coordinate system arises from the basis $\Phi_{r\theta}$. Consistent with the spatial decomposition method in [41], we will not elaborate much here, only give the relevant conclusions.

The normal form near the origin are governed by the following equations on its center manifold.

$$\begin{aligned}\dot{z}(t) &= \tilde{B}z(t) + \frac{1}{2}g_2^1(z,y,\mu) + \frac{1}{6}g_3^1(z,y,\mu) + h.o.t.,\\ \frac{\mathrm{d}y}{\mathrm{d}t} &= A_Q y + \frac{1}{2}g_2^2(z,y,\mu) + \frac{1}{6}g_3^2(z,y,\mu) + h.o.t.,\end{aligned}$$

where A_Q is the restriction of A on Q, for φ in Q, we can know $A_Q\varphi = A\varphi$, the projectionπ denote by $\pi : \mathscr{C} \to P_C$, in addition, $\tilde{B} = \mathrm{diag}(\mathrm{i}\boldsymbol{\omega}_{\hat{\lambda}}, -\mathrm{i}\boldsymbol{\omega}_{\hat{\lambda}}, \mathrm{i}\boldsymbol{\omega}_{\hat{\lambda}}, -\mathrm{i}\boldsymbol{\omega}_{\hat{\lambda}})$, the definition of $g = (g_j^1, g_j^2),\ j \geq 2$ is given in [41].

Thus, invariant local central manifolds are the following form,

$$\dot{z}(t) = \tilde{B}z(t) + \frac{1}{2}g_2^1(z,0,\mu) + \frac{1}{6}g_3^1(z,0,\mu) + \cdots .$$

In the next part, we now calculate the expression for $g_2^1(z,0,\mu)$ and $g_3^1(z,0,\mu)$, that is, calculate the following parameters.

$$\begin{aligned}B_{11} &= \frac{1}{2}\overline{\Psi_1(0)}(-\lambda_{mn}\tilde{D}_1\Phi_1(0) + \tilde{L}_1\Phi_1),\\ C_{2001} &= \frac{1}{6}\overline{\Psi_1(0)}A_{2001}\mathrm{M}_{22}, \qquad C_{1110} = \frac{1}{6}\overline{\Psi_1(0)}A_{1110}\mathrm{M}_{22},\\ E_{2001} &= \frac{1}{6}\overline{\Psi_1\,(0)}\left[\mathrm{M}^c_{0kcs}S_{yz_1}\left(h^{ccs}_{0k1001}\right) + \mathrm{M}^c_{2nkss}S_{yz_4}\left(h^{css}_{2nk2000}\right)\right],\\ E_{1110} &= \frac{1}{6}\overline{\Psi_1(0)}\left[M^c_{0kcs}(S_{yz_1}(h^{ccs}_{0k0110}) + S_{yz_2}(h^{ccs}_{0k1010})) + \mathrm{M}^c_{2nkss}S_{yz_3}(h^{css}_{2nk1100})\right],\\ B_{2001} &= C_{2001} + \frac{2}{3}E_{2001}, \qquad B_{1110} = C_{1110} + \frac{2}{3}E_{1110},\end{aligned}$$

where $\Psi_1(0), \tilde{D}_1, \tilde{L}_1, \Phi_1$ is given earlier in this section, and

$$\begin{aligned}&h^{ccs}_{0k1001}(\vartheta) = -\mathrm{M}^c_{0kcs}\left[-\lambda_{0k}\tilde{D}_0 + \tilde{L}_0(I_{\mathrm{d}})\right]^{-1}A_{1001}, \quad h^{ccs}_{0k0110}(\vartheta) = -\mathrm{M}^c_{0kcs}\left[-\lambda_{0k}\tilde{D}_0 + \tilde{L}_0(I_{\mathrm{d}})\right]^{-1}A_{0110},\\ &h^{ccs}_{0k1010}(\vartheta) = -\mathrm{M}^c_{0kcs}\mathrm{e}^{2\mathrm{i}\omega_{\hat{\lambda}}\vartheta}\left[-2\mathrm{i}\omega_{\hat{\lambda}} - \lambda_{0k}\tilde{D}_0 + \tilde{L}_0(\mathrm{e}^{2\mathrm{i}\omega_{\hat{\lambda}}}\cdot I_{\mathrm{d}})\right]^{-1}A_{1010},\\ &h^{ccs}_{2nk1100}(\vartheta) = -\mathrm{M}^s_{2nkcc}\left[-\lambda_{2nk}\tilde{D}_0 + \tilde{L}_0(I_d)\right]^{-1}A_{1100},\\ &h^{ccs}_{2nk2000}(\vartheta) = -\mathrm{M}^s_{2nkcc}\mathrm{e}^{2\mathrm{i}\omega_{\hat{\lambda}}\vartheta}\left[-2\mathrm{i}\omega_{\hat{\lambda}} - \lambda_{2nk}\tilde{D}_0 + \tilde{L}_0(\mathrm{e}^{2\mathrm{i}\omega_{\hat{\lambda}}}\cdot I_d)\right]^{-1}A_{2000},\\ &\mathrm{M}_{22} = \int_0^R\int_0^{2\pi} r\left(\hat{\phi}^c_{nm}\right)^2\left(\hat{\phi}^s_{nm}\right)^2\mathrm{d}\theta\mathrm{d}r, \quad \mathrm{M}^c_{0kcs} = \int_0^R\int_0^{2\pi} r\hat{\phi}_{jk}\hat{\phi}^c_{nm}\hat{\phi}^s_{nm}\mathrm{d}\theta\mathrm{d}r \text{ with } \hat{\phi}_{jk} = \hat{\phi}_0 \text{ or } \hat{\phi}^c_{0k},\\ &\mathrm{M}^c_{2nkss} = \int_0^R\int_0^{2\pi} r\hat{\phi}^c_{2nk}\hat{\phi}^s_{nm}\hat{\phi}^s_{nm}\mathrm{d}\theta\mathrm{d}r, \quad \mathrm{M}^s_{2nkcc} = \int_0^R\int_0^{2\pi} r\hat{\phi}^s_{2nk}\hat{\phi}^c_{nm}\hat{\phi}^c_{nm}\mathrm{d}\theta\mathrm{d}r,\\ &S_{yz_k}(\varphi) = S_{y(0)z_k}(\varphi(0)) + S_{y(-1)z_k}(\varphi(-1)),\ k = 1,2,3,4,\\ &A_{2000} = 2\tau^*\left(A^{(1)}_{2000}\ \ A^{(2)}_{2000}\ \ A^{(3)}_{2000}\right)^{\mathrm{T}}, \quad A_{1100} = 2\tau^*\left(A^{(1)}_{1100}\ \ A^{(2)}_{1100}\ \ A^{(3)}_{1100}\right)^{\mathrm{T}},\\ &A_{2001} = 6\tau^*\left(A^{(1)}_{2001}\ \ A^{(2)}_{2001}\ \ A^{(3)}_{2001}\right)^{\mathrm{T}},\\ &A_{1010} = 2A_{2000}, \quad A_{1001} = A_{1100}, \quad A_{0110} = \overline{A}_{1100}, \quad A_{1110} = 2A_{2001},\end{aligned}$$

with

$$S_{y(0)z_1}=S_{y(0)z_3}=\begin{pmatrix}2F_{200}^{(1)}+F_{110}^{(1)}p_1+F_{101}^{(1)}p_2 & 2F_{020}^{(1)}p_1+F_{110}^{(1)}+F_{011}^{(1)}p_2 & 2F_{002}^{(1)}p_2+F_{101}^{(1)}+F_{011}^{(1)}p_1\\ 2F_{200}^{(2)}+F_{110}^{(2)}p_1+F_{101}^{(2)}p_2 & 2F_{020}^{(2)}p_1+F_{110}^{(2)}+F_{011}^{(2)}p_2 & 2F_{002}^{(2)}p_2+F_{101}^{(2)}+F_{011}^{(2)}p_1\\ 0 & 0 & 2F_{002}^{(3)}p_2+F_{101}^{(3)}e^{-\mathrm{i}\omega_{\hat{\lambda}}\tau^*}+F_{011}^{(2)}p_1e^{-\mathrm{i}\omega_{\hat{\lambda}}\tau^*}\end{pmatrix},$$

$$S_{y(0)z_2}=S_{y(0)z_4}=\begin{pmatrix}2F_{200}^{(1)}+F_{110}^{(1)}\overline{p}_1+F_{101}^{(1)}\overline{p}_2 & 2F_{020}^{(1)}\overline{p}_1+F_{110}^{(1)}+F_{011}^{(1)}\overline{p}_2 & 2F_{002}^{(1)}\overline{p}_2+F_{101}^{(1)}+F_{011}^{(1)}\overline{p}_1\\ 2F_{200}^{(2)}+F_{110}^{(2)}\overline{p}_1+F_{101}^{(2)}\overline{p}_2 & 2F_{020}^{(2)}\overline{p}_1+F_{110}^{(2)}+F_{011}^{(2)}\overline{p}_2 & 2F_{002}^{(2)}\overline{p}_2+F_{101}^{(2)}+F_{011}^{(2)}\overline{p}_1\\ 0 & 0 & 2F_{002}^{(3)}\overline{p}_2+F_{101}^{(3)}e^{\mathrm{i}\omega_{\hat{\lambda}}\tau^*}+F_{011}^{(2)}\overline{p}_1e^{\mathrm{i}\omega_{\hat{\lambda}}\tau^*}\end{pmatrix},$$

$$S_{y(-1)z_1}=S_{y(-1)z_3}=\begin{pmatrix}0 & 0 & 0\\ 0 & 0 & 0\\ 2F_{200}^{(3)}e^{-\mathrm{i}\omega_{\hat{\lambda}}\tau^*}+F_{110}^{(3)}p_1e^{-\mathrm{i}\omega_{\hat{\lambda}}\tau^*}+F_{101}^{(3)}p_2 & 2F_{020}^{(3)}p_1e^{-\mathrm{i}\omega_{\hat{\lambda}}\tau^*}+F_{110}^{(3)}e^{-\mathrm{i}\omega_{\hat{\lambda}}\tau^*}+F_{011}^{(3)}p_2 & 0\end{pmatrix},$$

$$S_{y(-1)z_2}=S_{y(-1)z_4}=\begin{pmatrix}0 & 0 & 0\\ 0 & 0 & 0\\ 2F_{200}^{(3)}e^{\mathrm{i}\omega_{\hat{\lambda}}\tau^*}+F_{110}^{(3)}\overline{p}_1e^{\mathrm{i}\omega_{\hat{\lambda}}\tau^*}+F_{101}^{(3)}\overline{p}_2 & 2F_{020}^{(3)}\overline{p}_1e^{\mathrm{i}\omega_{\hat{\lambda}}\tau^*}+F_{110}^{(3)}e^{\mathrm{i}\omega_{\hat{\lambda}}\tau^*}+F_{011}^{(3)}\overline{p}_2 & 0\end{pmatrix},$$

$$\begin{aligned}
A_{2000}^{(1)}=&F_{200}^{(1)}+F_{020}^{(1)}p_1^2+F_{002}^{(1)}p_2^2+F_{110}^{(1)}p_1+F_{101}^{(1)}p_2+F_{011}^{(1)}p_1p_2,\\
A_{2000}^{(2)}=&F_{200}^{(2)}+F_{020}^{(2)}p_1^2+F_{002}^{(2)}p_2^2+F_{110}^{(2)}p_1+F_{101}^{(2)}p_2+F_{011}^{(2)}p_1p_2,\\
A_{2000}^{(3)}=&F_{200}^{(3)}e^{-2\mathrm{i}\omega_{\hat{\lambda}}\tau^*}+F_{020}^{(3)}p_1^2e^{-2\mathrm{i}\omega_{\hat{\lambda}}\tau^*}+F_{002}^{(3)}p_2^2+F_{110}^{(3)}p_1e^{-\mathrm{i}\omega_{\hat{\lambda}}\tau^*}+F_{101}^{(3)}p_2e^{-\mathrm{i}\omega_{\hat{\lambda}}\tau^*}+F_{011}^{(3)}p_1p_2e^{-\mathrm{i}\omega_{\hat{\lambda}}\tau^*},\\
A_{1100}^{(1)}=&2F_{200}^{(1)}+2F_{020}^{(1)}p_1\overline{p}_1+2F_{002}^{(1)}p_2\overline{p}_2+F_{110}^{(1)}(p_1+\overline{p}_1)+F_{101}^{(1)}(p_2+\overline{p}_2)+F_{011}^{(1)}(p_1\overline{p}_2+\overline{p}_1p_2),\\
A_{1100}^{(2)}=&2F_{200}^{(2)}+2F_{020}^{(2)}p_1\overline{p}_1+2F_{002}^{(2)}p_2\overline{p}_2+F_{110}^{(2)}(p_1+\overline{p}_1)+F_{101}^{(2)}(p_2+\overline{p}_2)+F_{011}^{(2)}(p_1\overline{p}_2+\overline{p}_1p_2),\\
A_{1100}^{(3)}=&2F_{200}^{(3)}+2F_{020}^{(3)}p_1\overline{p}_1+2F_{002}^{(3)}p_2\overline{p}_2+F_{110}^{(3)}(p_1+\overline{p}_1)+F_{101}^{(3)}(p_2e^{\mathrm{i}\omega_{\hat{\lambda}}\tau^*}+\overline{p}_2e^{-\mathrm{i}\omega_{\hat{\lambda}}\tau^*})\\
&+F_{011}^{(3)}(p_1\overline{p}_2e^{-\mathrm{i}\omega_{\hat{\lambda}}\tau^*}+\overline{p}_1p_2e^{\mathrm{i}\omega_{\hat{\lambda}}\tau^*}),\\
A_{2001}^{(1)}=&3F_{300}^{(1)}+3F_{030}^{(1)}p_1^2\overline{p}_1+3F_{003}^{(1)}p_2^2\overline{p}_2+F_{210}^{(1)}(2p_1+\overline{p}_1)+F_{201}^{(1)}(2p_2+\overline{p}_2)+F_{120}^{(1)}(p_1^2+2p_1\overline{p}_1)\\
&+F_{102}^{(1)}(p_2^2+2p_2\overline{p}_2)+F_{021}^{(1)}(p_1^2\overline{p}_2+2p_1\overline{p}_1p_2)+F_{012}^{(1)}(p_2^2\overline{p}_1+2p_1\overline{p}_2p_2)+F_{111}^{(1)}(p_1p_2+\overline{p}_1p_2+\overline{p}_2p_1),\\
A_{2001}^{(2)}=&3F_{300}^{(2)}+3F_{030}^{(2)}p_1^2\overline{p}_1+3F_{003}^{(2)}p_2^2\overline{p}_2+F_{210}^{(2)}(2p_1+\overline{p}_1)+F_{201}^{(2)}(2p_2+\overline{p}_2)+F_{120}^{(2)}(p_1^2+2p_1\overline{p}_1)\\
&+F_{102}^{(2)}(p_2^2+2p_2\overline{p}_2)+F_{021}^{(2)}(p_1^2\overline{p}_2+2p_1\overline{p}_1p_2)+F_{012}^{(2)}(p_2^2\overline{p}_1+2p_1\overline{p}_2p_2)+F_{111}^{(2)}(p_1p_2+\overline{p}_1p_2+\overline{p}_2p_1),\\
A_{2001}^{(3)}=&3F_{300}^{(3)}e^{-\mathrm{i}\omega_{\hat{\lambda}}\tau^*}+3F_{030}^{(2)}p_1^2\overline{p}_1e^{-\mathrm{i}\omega_{\hat{\lambda}}\tau^*}+3F_{003}^{(3)}p_2^2\overline{p}_2+F_{210}^{(3)}(2p_1+\overline{p}_1)e^{-\mathrm{i}\omega_{\hat{\lambda}}\tau^*}+F_{201}^{(3)}(2p_2+\overline{p}_2e^{-2\mathrm{i}\omega_{\hat{\lambda}}\tau^*})\\
&+F_{120}^{(3)}(p_1^2+2p_1\overline{p}_1)e^{-\mathrm{i}\omega_{\hat{\lambda}}\tau^*}+F_{102}^{(3)}(p_2^2e^{\mathrm{i}\omega_{\hat{\lambda}}\tau^*}+2p_2\overline{p}_2e^{-\mathrm{i}\omega_{\hat{\lambda}}\tau^*})+F_{021}^{(3)}(p_1^2\overline{p}_2e^{-2\mathrm{i}\omega_{\hat{\lambda}}\tau^*}+2p_1\overline{p}_1p_2)\\
&+F_{012}^{(3)}(p_2^2\overline{p}_1e^{\mathrm{i}\omega_{\hat{\lambda}}\tau^*}+2p_1\overline{p}_2p_2e^{-\mathrm{i}\omega_{\hat{\lambda}}\tau^*})+F_{111}^{(3)}(p_1p_2+\overline{p}_1p_2+\overline{p}_2p_1e^{-2\mathrm{i}\omega_{\hat{\lambda}}\tau^*}).
\end{aligned}$$

Thereby, the normal form at the equivariant Hopf bifurcation point can be obtained,

$$\begin{cases} \dot{z}_1 = \mathrm{i}\omega_{\hat{\lambda}} z_1 + B_{11} z_1 \mu + B_{2001} z_1^2 z_4 + B_{1110} z_1 z_2 z_3, \\ \dot{z}_2 = -\mathrm{i}\omega_{\hat{\lambda}} z_2 + \overline{B_{11}} z_2 \mu + \overline{B_{2001}} z_3 z_2^2 + \overline{B_{1110}} z_1 z_2 z_4, \\ \dot{z}_3 = \mathrm{i}\omega_{\hat{\lambda}} z_3 + B_{11} z_3 \mu + B_{2001} z_3^2 z_2 + B_{1110} z_1 z_3 z_4, \\ \dot{z}_4 = -\mathrm{i}\omega_{\hat{\lambda}} z_4 + \overline{B_{11}} z_4 \mu + \overline{B_{2001}} z_1 z_4^2 + \overline{B_{1110}} z_2 z_3 z_4. \end{cases}$$

The third-order truncated normal form on the center manifold admits the following form when expressed in double polar coordinates,

$$\begin{cases} \dot{\rho}_1 = \left(a_1 \mu + a_2 \rho_1^2 + a_3 \rho_2^2\right) \rho_1, \\ \dot{\chi}_1 = \omega_{\hat{\lambda}}, \\ \dot{\rho}_2 = \left(a_1 \mu + a_2 \rho_2^2 + a_3 \rho_1^2\right) \rho_2, \\ \dot{\chi}_2 = \omega_{\hat{\lambda}}, \end{cases}$$

with

$$a_1 = \mathrm{Re}\{B_{11}\},\ a_2 = \mathrm{Re}\{B_{2001}\},\ a_3 = \mathrm{Re}\{B_{1110}\}.$$

According to the sign of $a_2,\ a_2 + a_3,\ a_2 - a_3$, the unfoldings of the system can be divided into six types (see [41] for details), therefore, the system has six different dynamic patterns when $a_1\mu < 0$ and $a_1\mu > 0$, respectively, which we will explain this in the next section with actual data.

4. Numerical simulations

In this section, some numerical simulations of system are given to verify the theoretical results in the previous sections. The parameter values except the diffusion coefficients are selected from [34] directly used by us, and the data in [34] is aggregated from [25, 57, 58], where data can reflect certain biological phenomena in reality.

Let's start with the first set of simulations, choose the parameter set

$$\begin{aligned} \text{(i)}\ & r_1 = 0.46, \quad r_2 = 0.44, \quad K_1 = 500, \quad K_2 = 500, \quad a_1 = 0.0002, \quad a_2 = 0.0001, \quad b_1 = 0.6, \\ & b_2 = 0.4, \quad c_1 = 50, \quad c_2 = 30, \quad \alpha = 0.8, \quad \beta = 0.5, \quad A = 10, \quad \theta_1 = 0.5, \\ & \theta_2 = 0.49, \quad \delta = 0.3, \quad e_1 = 0.5, \quad e_2 = 0.35, \quad d_1 = 0.309, \quad d_2 = 0.002, \\ & D_1 = 0.8, \quad D_2 = 0.6, \quad D_3 = 0.5, \quad \chi_1 = 0.01. \end{aligned}$$

For the unique spatially uniform positive stationary state, a subset of bifurcation curves in the $\chi_2 - \tau$ parameter space is illustrated in Figure 1, the bifurcation curves show the concrete manifestation of the stable switch mentioned in Theorem 3.6 in Section 3. The blue line $\tau_{\lambda_{00}}$ indicates the bifurcation curve corresponding to $n = 0,\ m = 0$, since $\lambda_{00} = 0$, the curve is horizontal, that is, it does not change with the increase of the taxic term χ_2; the red line $\tau_{\lambda_{11}}$ indicates the bifurcation curve corresponding to $n = 1,\ m = 1$; and the yellow line $\tau_{\lambda_{21}}$ indicates the bifurcation curve corresponding to $n = 2,\ m = 1$, these two lines are curved in form due to the presence of the stability switch. Moreover, as the parameter χ_2 changes, a double Hopf point EH-EH arises, which we can see from Figure 1. Specifically, this corresponds to the scenario where the characteristic equation (3.5) possesses two pairs of double conjugate purely imaginary roots, leading to the simultaneous emergence of two equivariant Hopf bifurcations. Such a phenomenon represents a more intricate bifurcation scenario, which must be investigated on an eight-dimensional central manifold.

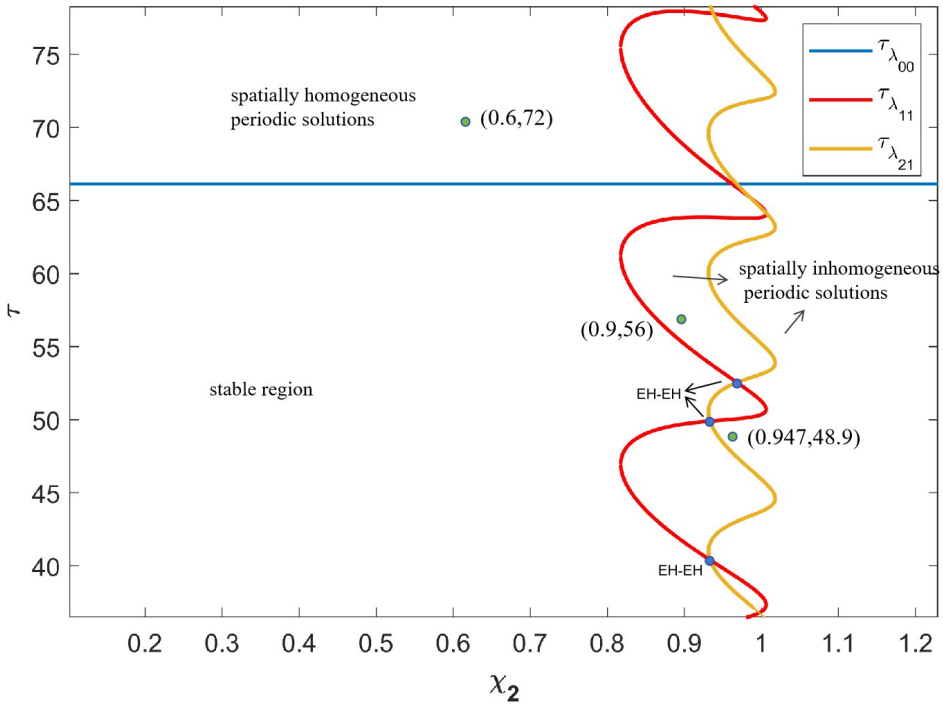

FIGURE 1. Partial bifurcation curves on the $\chi_2 - \tau$ plane. We choose parameters values are given in (i).

We select the point $(\chi_2, \tau) = (0.6, 72)$ in Figure 1. At this time $\hat{\lambda} = \lambda_{00}$, the Hopf bifurcation occurs at $\tau^* = \tau_{\lambda_{00}} \approx 66.1468$. The equilibrium E^* maintains local asymptotic stability for delay values within $\tau \in [0,\ 66.1468)$. This is the stable region shown in Figure 1. Beyond the critical threshold $\tau^* \approx 66.1468$, a family of spatially homogeneous periodic solutions generate from E^* (visualized in Fig. 2). By concrete numerical calculation, we know that $a_1^* a_2^* \approx -0.6799$, $a_2^* \approx -0.3420$, signifying a supercritical Hopf bifurcation. Consequently, the resulting periodic orbits exhibit stability.

Then we choose the point $(\chi_2, \tau) = (0.9, 56)$ in Figure 1, equivariant Hopf bifurcation occurs at $\tau_{\lambda_{11}} \approx 55.1813$. Numerical computations confirm that $\mu = 0.8171$, $B_{11} \approx 0.0162 - 0.2640\mathrm{i}$, $B_{2001} \approx 0.0368 + 0.054\mathrm{i}$, $B_{1110} \approx 0.0184 + 0.0270\mathrm{i}$. Thus, $a_1\mu \approx -0.01328586$, $a_2 \approx 0.036849$, $a_2 + a_3 \approx 0.055274$, $a_2 - a_3 \approx 0.018425$, following the classification in [41] [Table 2, Case 5: $a_1\mu < 0$]. This parameter configuration induces an unstable standing wave (Fig. 3) and two unstable rotating waves (Fig. 4), since the three variables of P, H, Z change synchronously, for the sake of simplicity, we will only give the patterns of two rotating waves of P, which is the same as below.

Finally we choose the point $(\chi_2, \tau) = (0.947, 48.9)$ in Figure 1, which means equivariant Hopf bifurcation generate at $\tau_{\lambda_{21}} \approx 48.6409$. In this instance, $\mu = 0.2291$, $B_{11} \approx -0.3264 - 0.3791\mathrm{i}$, $B_{2001} \approx 0.0131 + 0.0595\mathrm{i}$, $B_{1110} \approx 0.0262 + 0.1189\mathrm{i}$. Thus, $a_1\mu \approx -0.0747789$, $a_2 \approx 0.013088$, $a_2 + a_3 \approx 0.039263$, $a_2 - a_3 \approx -0.013088$, which corresponds to Case 6 when $a_1\mu < 0$, and the parameter constellation predicts bifurcation dynamics in (1.2) featuring an unstable standing wave (Fig. 5) and two unstable rotating waves (Fig. 6).

Next we run a second set of simulations, choose the following parameter set

$$\begin{aligned}
\text{(ii)}\ & r_1 = 0.46, \quad r_2 = 0.44, \quad K_1 = 500, \quad K_2 = 500, \quad a_1 = 0.0002, \quad a_2 = 0.0001, \quad b_1 = 0.6, \\
& b_2 = 0.4, \quad c_1 = 50, \quad c_2 = 30, \quad \alpha = 0.8, \quad \beta = 0.5, \quad A = 10, \quad \theta_1 = 0.5, \\
& \theta_2 = 0.49, \quad \delta = 0.3, \quad e_1 = 0.5, \quad e_2 = 0.35, \quad d_1 = 0.309, \quad d_2 = 0.0082, \\
& D_1 = 0.8, \quad D_2 = 0.6, \quad D_3 = 0.5, \quad \chi_1 = 0.01.
\end{aligned}$$

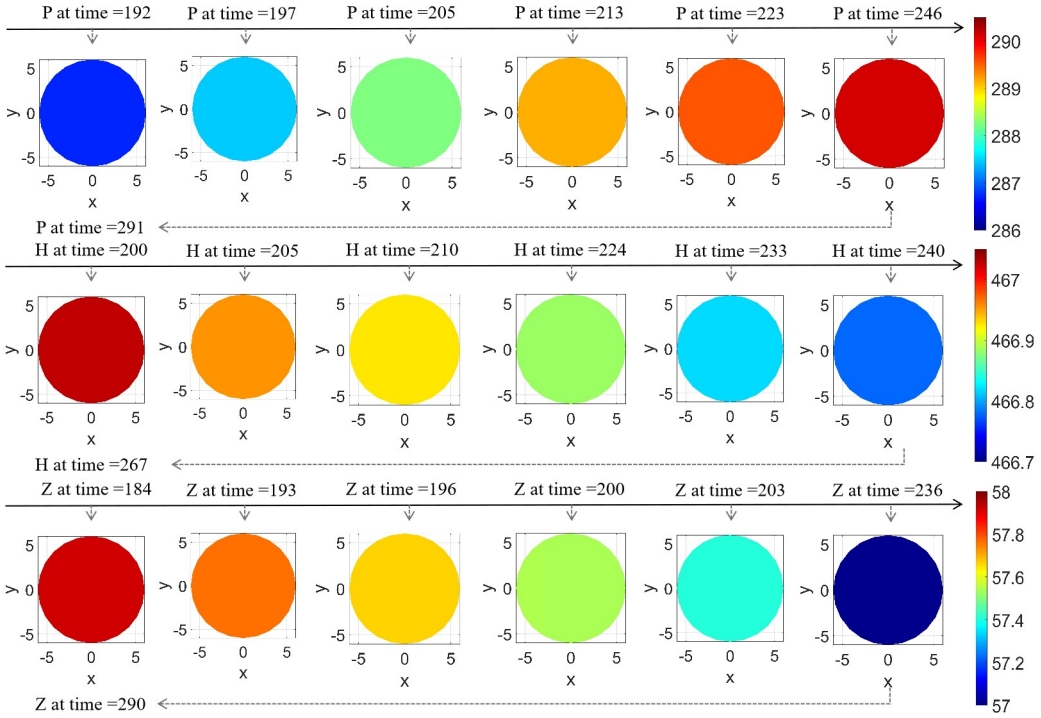

FIGURE 2. Spatially homogeneous periodic solutions with parameters given in(i).

Using the same way, we can get the partial bifurcation curves on the $\chi_2 - \tau$ plane that are shown in Figure 7, with variations in the parameter χ_2, a double Hopf bifurcation point H-EH emerges, as illustrated in Figure 7. More precisely, this occurs when the characteristic equation (3.4) exhibits a pair of simple conjugate purely imaginary roots and (3.5) exhibits a pair of complex conjugate purely imaginary roots. Such a configuration reflects a higher-order bifurcation dynamic, necessitating analysis on a six-dimensional central manifold to fully characterize the system's behavior.

Additionally, we select the point $(\chi_2, \tau) = (0.31, 0.2)$ on the plane of $\chi_2 - \tau$. Equivariant Hopf bifurcation occurs at $\tau_{\lambda_{11}} \approx 0.187575$. At the present moment, the system (1.2) exhibits an unstable standing wave (Fig. 8) and two unstable rotating waves (Figs. 9 and 10) with $B_{11} \approx -0.1766 - 0.1264\mathrm{i}$, $B_{2001} \approx 0.0262 + 0.0677\mathrm{i}$, $B_{1110} \approx 0.0577 + 0.1564\mathrm{i}$. Thus, $a_1\mu \approx -0.002194$, $a_2 \approx 0.026183$, $a_2 + a_3 \approx 0.083840$, $a_2 - a_3 \approx -0.031474$, which corresponds to Case 6 when $a_1\mu < 0$.

At the point $(\chi_2, \tau) = (0.4, 34)$ on the plane of $\chi_2 - \tau$, the equivariant Hopf bifurcation occurs at $\tau_{\lambda_{11}} \approx 33.4222$. It can be obtained through numerical calculations that $\mu = 0.5778$, $B_{11} \approx 0.0567 - 0.0232\mathrm{i}$, $B_{2001} \approx -0.0057 - 0.0027\mathrm{i}$, $B_{1110} \approx -0.0114 - 0.0055\mathrm{i}$. Thus, $a_1\mu \approx 0.03275086$, $a_2 \approx -0.005715$, $a_2 + a_3 \approx -0.017145$, $a_2 - a_3 \approx 0.005715$, which corresponds to Case 2 when $a_1\mu > 0$. As a result, the system (1.2) demonstrates an unstable standing wave (Fig. 11) and two asymptotically stable rotating waves (Fig. 12).

Based on the two sets of numerical simulations, we observe that both standing waves and rotating waves represent spatially inhomogeneous periodic solutions, each capturing the cyclic population dynamics of the three species-NTP, TPP, and zooplankton. However, their distinct solution types reflect different outcomes of species interactions. Specifically, as illustrated in the figures (Figs. 3 and 5), standing waves exhibit regions of constant coloration, indicating the formation of localized areas within the two-dimensional circular domain where population densities remain constant over time. In these subregions, the populations demonstrate stable coexistence, while periodic oscillations occur elsewhere. In contrast, rotating waves do not yield such stationary

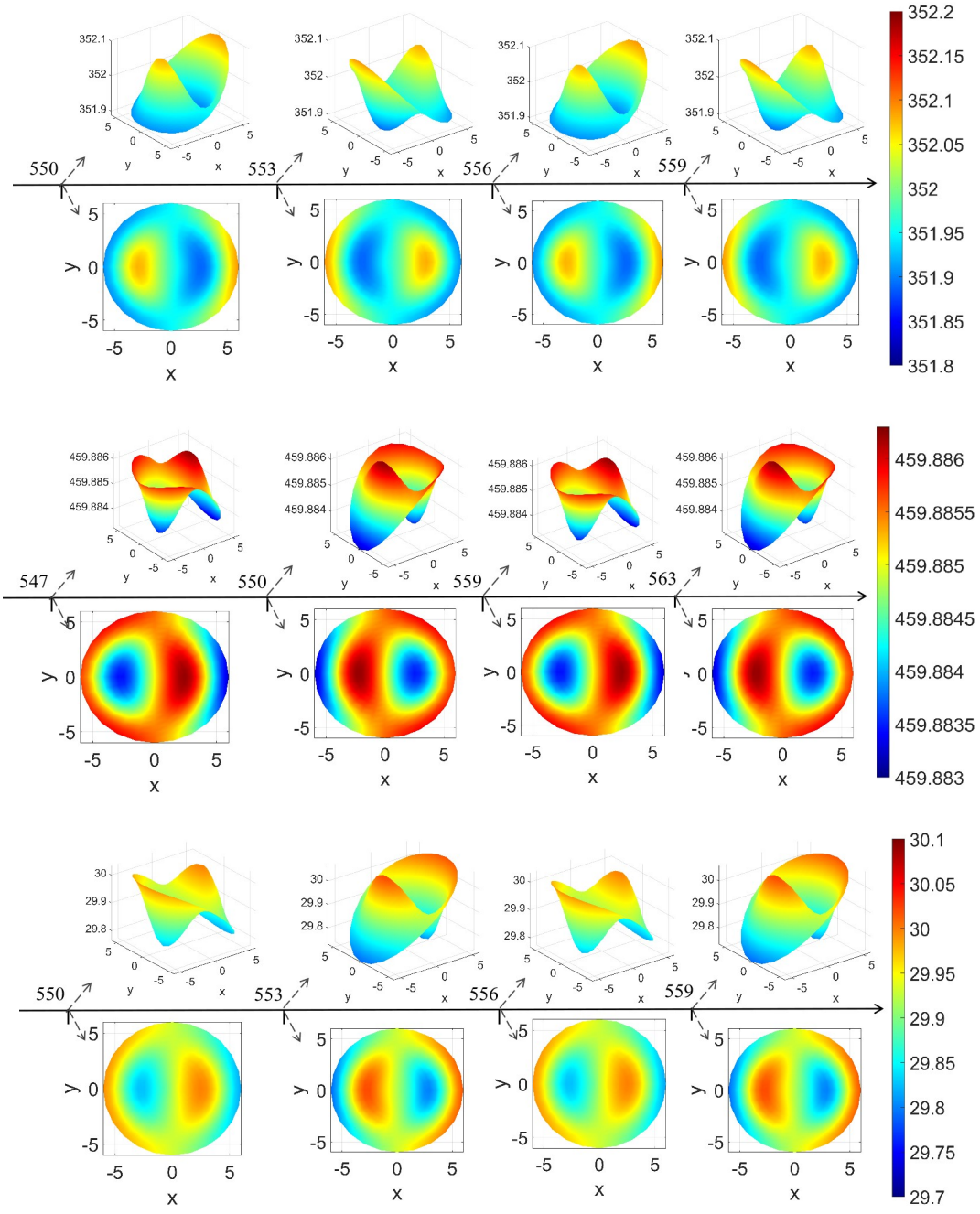

FIGURE 3. The system exhibits standing waves with parameter values that are given in (i) at the point $(\chi_2, \tau) = (0.9, 56)$ in Figure 1, initial values are $P(r,\theta,t) = 288.2573 + 2 \cdot \cos r \cdot \cos\theta \cdot \cos t$, $H(r,\theta,t) = 466.9979 + 3 \cdot \cos r \cdot \cos\theta \cdot \cos t$, $Z(r,\theta,t) = 57.8434 + 1 \cdot \cos r \cdot \cos\theta \cdot \cos t$, the picture shows the pattern of P, H, Z from top to bottom.

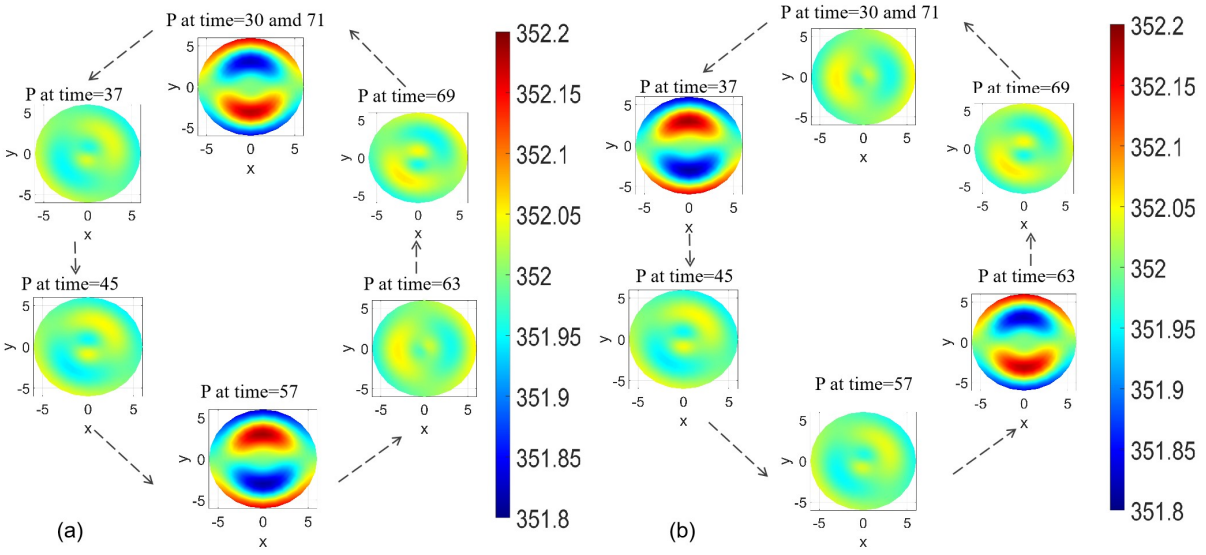

FIGURE 4. The system exhibits rotating waves with parameter values given in (i) at the point $(\chi_2, \tau) = (0.9, 56)$ in Figure 1, (a) initial values are $P(r,\theta,t) = 288.2573 + 1 \cdot \cos r \cdot \cos\theta \cdot \cos t$, $H(r,\theta,t) = 466.9979 + 1 \cdot \cos r \cdot \sin\theta \cdot \cos t$, $Z(r,\theta,t) = 57.8434 + 1 \cdot \cos r \cdot \cos\theta \cdot \cos t$; (b) initial values are $P(r,\theta,t) = 288.2573 + 1 \cdot \cos r \cdot \sin\theta \cdot \cos t$, $H(r,\theta,t) = 466.9979 + 1 \cdot \cos r \cdot \cos\theta \cdot \cos t$, $Z(r,\theta,t) = 57.8434 + 1 \cdot \cos r \cdot \cos\theta \cdot \cos t$.

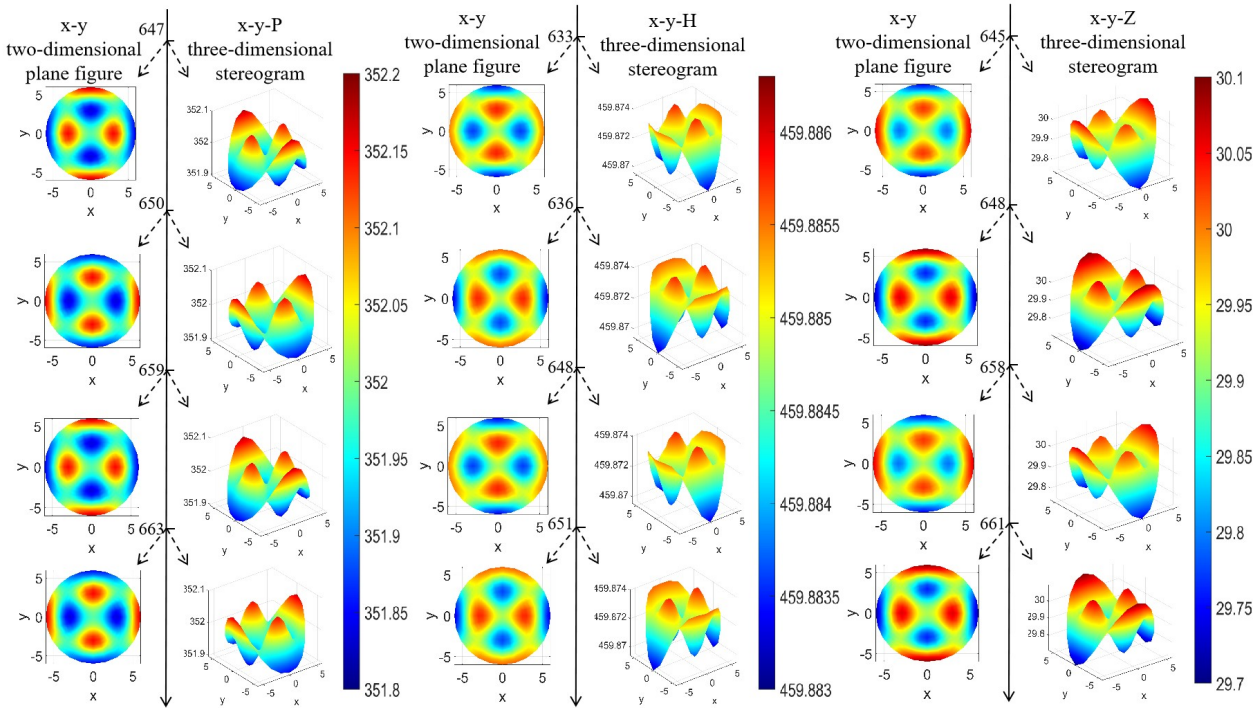

FIGURE 5. The system exhibits standing waves with parameter values given in (ii) at the point $(\chi_2, \tau) = (0.947, 48.9)$ in Figure 1, initial values are $P(r,\theta,t) = 288.2573 + 2 \cdot \cos r \cdot \cos 2\theta \cdot \cos t$, $H(r,\theta,t) = 466.9979 + 3 \cdot \cos r \cdot \cos 2\theta \cdot \cos t$, $Z(r,\theta,t) = 57.8434 + 1 \cdot \cos r \cdot \cos 2\theta \cdot \cos t$.

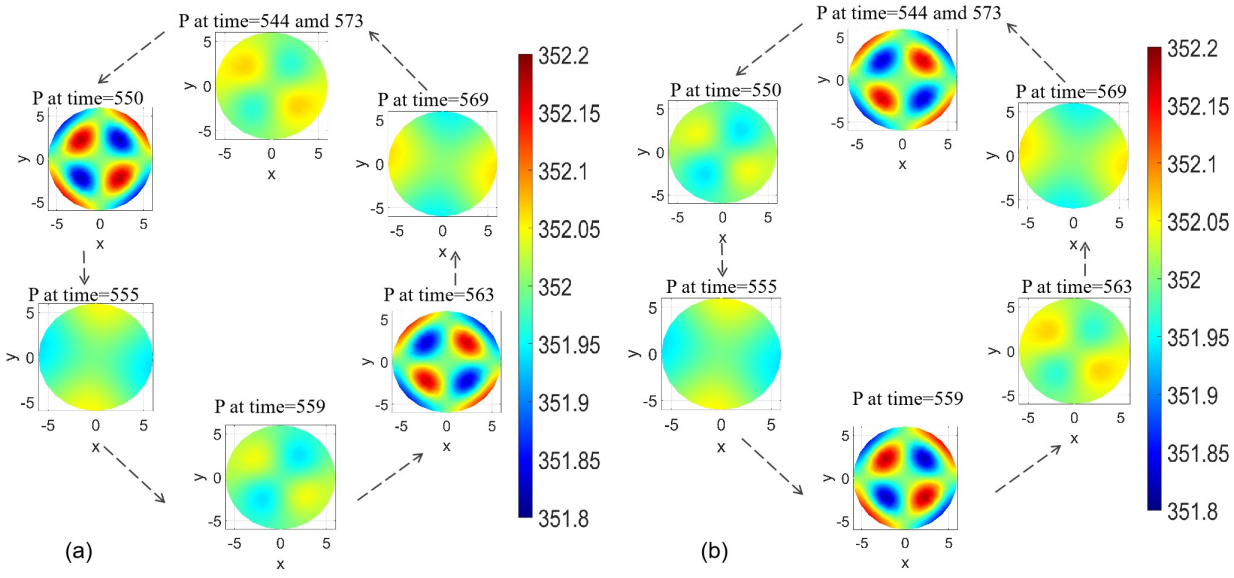

FIGURE 6. The system demonstrates rotating waves with parameter values given in (i) at the point $(\chi_2, \tau) = (0.947, 48.9)$ in Figure 1, (a) initial values are $P(r,\theta,t) = 288.2573 + 1 \cdot \cos r \cdot \sin 2\theta \cdot \cos t$, $H(r,\theta,t) = 466.9979 + 1 \cdot \cos r \cdot \sin 2\theta \cdot \cos t$, $Z(r,\theta,t) = 57.8434 + 1 \cdot \cos r \cdot \cos 2\theta \cdot \cos t$; (b) initial values are $P(r,\theta,t) = 288.2573 + 1 \cdot \cos r \cdot \sin 2\theta \cdot \cos t$, $H(r,\theta,t) = 466.9979 + 1 \cdot \cos r \cdot \cos 2\theta \cdot \cos t$, $Z(r,\theta,t) = 57.8434 + 1 \cdot \cos r \cdot \sin 2\theta \cdot \cos t$.

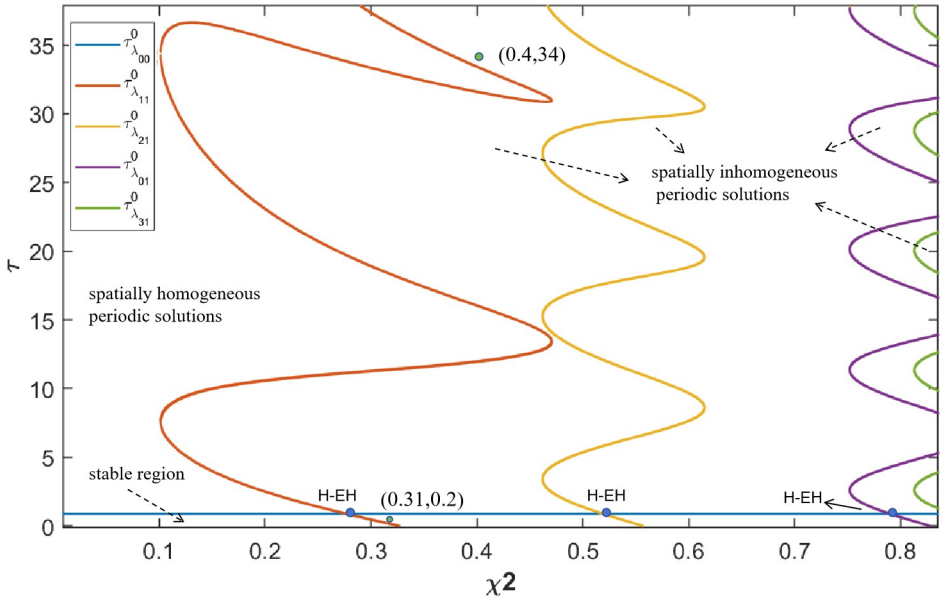

FIGURE 7. Partial bifurcation curves on the $\chi_2 - \tau$ plane. We choose parameters values that are given in (ii).

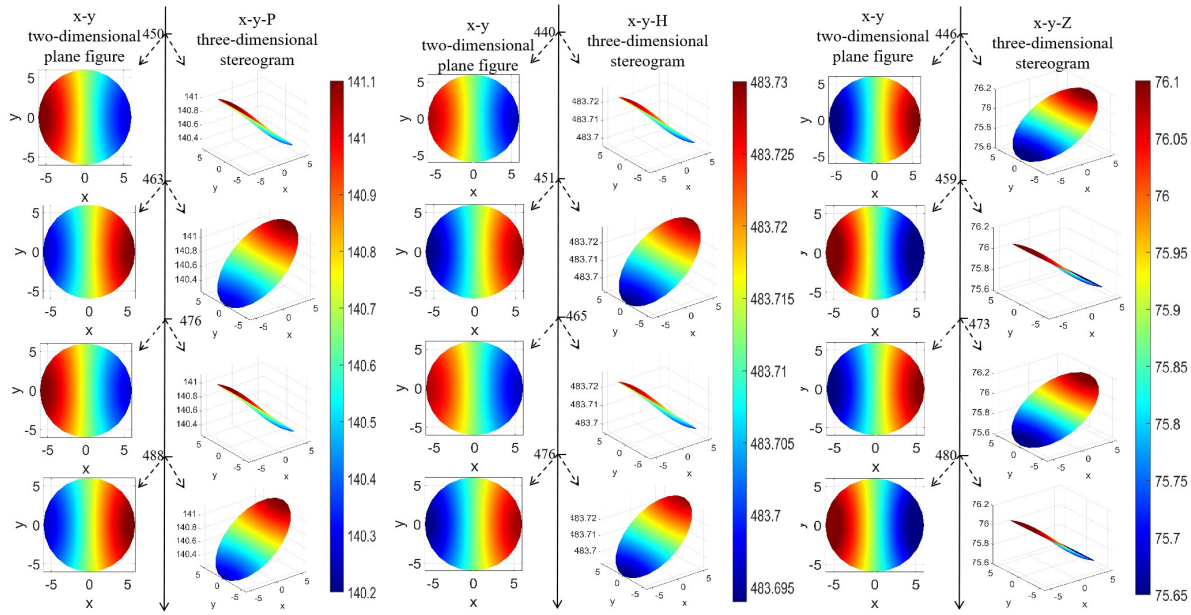

FIGURE 8. The system produces standing waves with parameter values given in (ii) at the point $(\chi_2, \tau) = (0.31, 0.2)$ in Figure 7, initial values are $P(r,\theta,t) = 140.6880 + 10 \cdot \cos r \cdot \cos\theta \cdot \cos t$, $H(r,\theta,t) = 483.7122 + 10 \cdot \cos r \cdot \cos\theta \cdot \cos t$, $Z(r,\theta,t) = 75.8713 + 10 \cdot \cos r \cdot \cos\theta \cdot \cos t$.

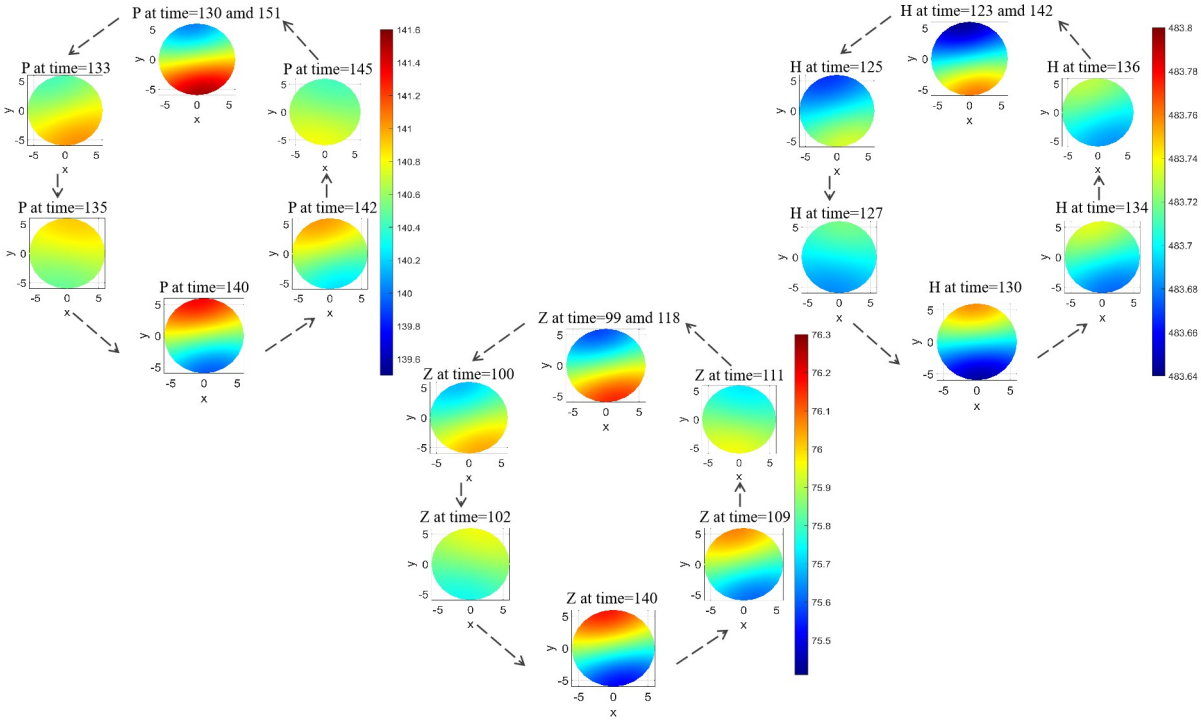

FIGURE 9. The system demonstrates rotating waves with parameter values given in (ii) at the point $(\chi_2, \tau) = (0.31, 0.2)$ in Figure 7, initial values are $P(r,\theta,t) = 140.6880 + 10 \cdot \cos r \cdot \sin\theta \cdot \cos t$, $H(r,\theta,t) = 483.7122 + 10 \cdot \cos r \cdot \cos\theta \cdot \cos t$, $Z(r,\theta,t) = 75.8713 + 10 \cdot \cos r \cdot \sin\theta \cdot \cos t$.

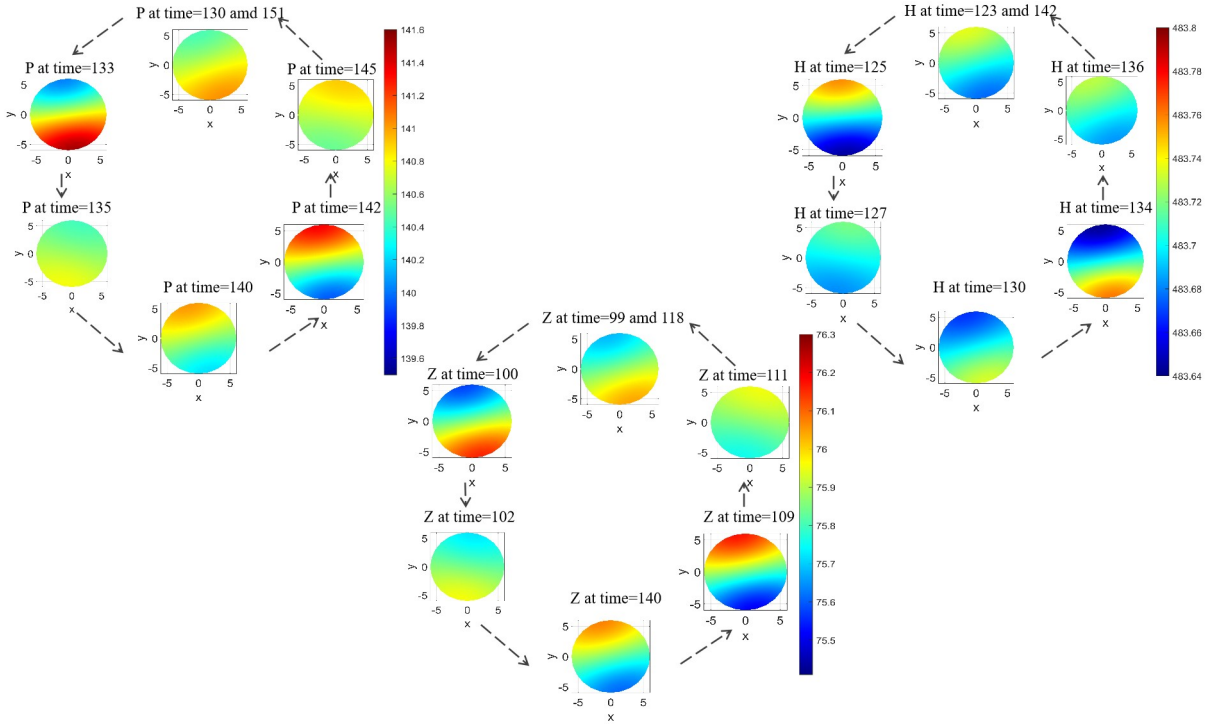

FIGURE 10. The system produces rotating waves with parameter values given in (ii) at the point $(\chi_2, \tau) = (0.31, 0.2)$ in Figure 7, initial values are $P(r,\theta,t) = 140.6880 + 10 \cdot \cos r \cdot \cos\theta \cdot \cos t$, $H(r,\theta,t) = 483.7122 + 10 \cdot \cos r \cdot \sin\theta \cdot \cos t$, $Z(r,\theta,t) = 75.8713 + 10 \cdot \cos r \cdot \sin\theta \cdot \cos t$.

coexistence in any fixed region; instead, zones of high and low population density continuously shift across the domain. This spatial movement prevents local overpopulation or extinction extremes in any given area. We argue that both types of spatially inhomogeneous periodic solutions imply continuously shifting hotspots of population density, which prevents any single species from dominating a specific region over extended periods, thereby promoting the coexistence of all species.

It is not difficult to find that the difference between the two sets of simulations is that we changed the cannibalism rate of zooplankton d_2. In addition, after more simulation experiments, we give the corresponding bifurcation curves when $d_2 = 0.001$. Compared with Figures 1, 7 and 13, we can find that higher cannibalism ability of zooplankton has an enhanced effect on the stability of the system (1.2), also can indirectly lead to an overabundance of phytoplankton and allow phytoplankton populations to reach their environmental capacity. But excessive cannibalism can cause zooplankton populations to plummet and even become extinct. This is the enrichment paradox in ecology. Furthermore, we change other parameters, such as additional food coefficient A, the Allee effect coefficient δ, and the various diffusion coefficients D_1, D_2, D_3 and χ_1, then we get more complex and different pictures of bifurcation curves (see Fig. 14a and b). This also shows that changes of cannibalism, Allee effect, grazing selectivity and additional food can lead to changes in spatial patterns and produce different periodic phenomena.

In addition, in view of the bifurcation curves, we can also find that the system will produce standing and rotating waves and more complex dynamic behaviors as the taxic term coefficient χ_2 increases in the lateral direction, that is, the x-axis direction. From the perspective of longitudinal, that is, y-axis, with the increase of time delay, the system will produce spatial homogeneous periodic solutions. In this three-species model incorporating chemotaxis, the bifurcation diagram reveals that with an appropriate increase in the chemotaxis

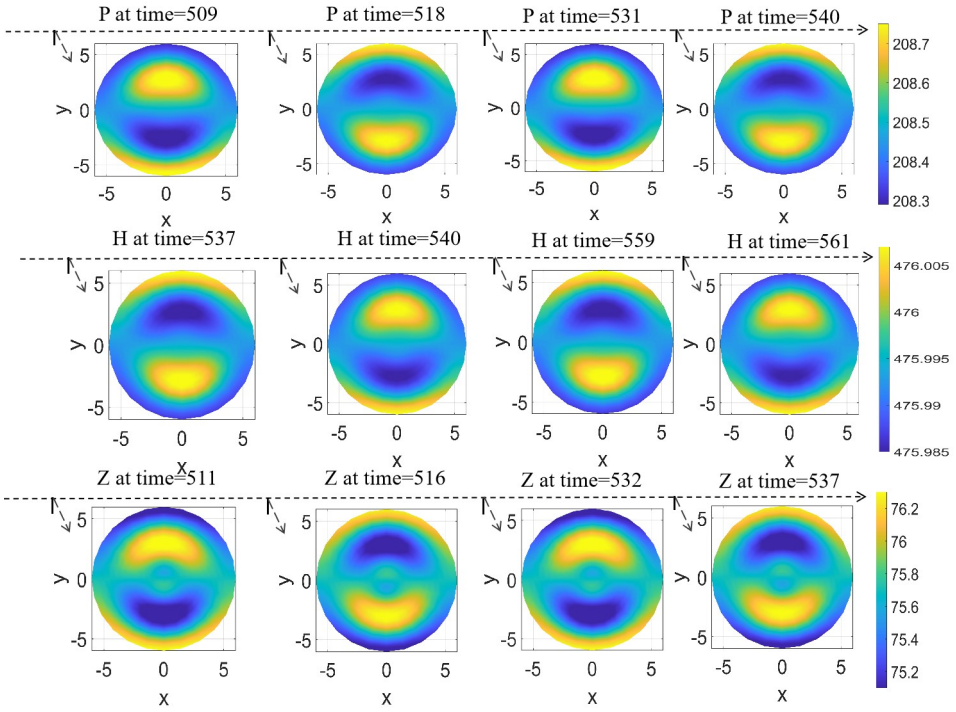

FIGURE 11. The system produces standing waves with parameter values given in (ii) at the point $(\chi_2, \tau) = (0.4, 34)$ in Figure 7, initial values are $P(r,\theta,t) = 140.6880 + 20 \cdot \cos r \cdot \cos(\theta - \pi/2) \cdot \cos t$, $H(r,\theta,t) = 483.7122 + 30 \cdot \cos r \cdot \cos(\theta - \pi/2) \cdot \cos t$, $Z(r,\theta,t) = 75.8713 + 10 \cdot \cos r \cdot \cos(\theta - \pi/2) \cdot \cos t$.

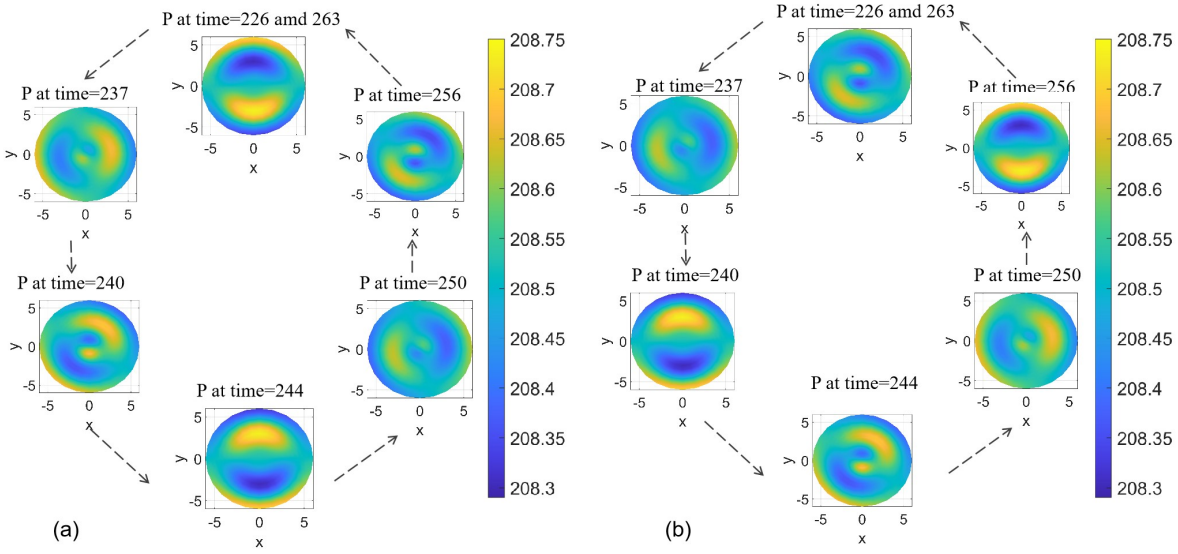

FIGURE 12. The system produces rotating waves with parameter values given in (ii) at the point $(\chi_2, \tau) = (0.4, 34)$ in Figure 7: (a) initial values are $P(r,\theta,t) = 140.6880 + 1 \cdot \cos r \cdot \cos\theta \cdot \cos t$, $H(r,\theta,t) = 483.7122 + 1 \cdot \cos r \cdot \sin\theta \cdot \cos t$, $Z(r,\theta,t) = 75.8713 + 1 \cdot \cos r \cdot \sin\theta \cdot \cos t$; (b) initial values are $P(r,\theta,t) = 140.6880 + 1 \cdot \cos r \cdot \sin\theta \cdot \cos t$, $H(r,\theta,t) = 483.7122 + 1 \cdot \cos r \cdot \sin\theta \cdot \cos t$, $Z(r,\theta,t) = 75.8713 + 1 \cdot \cos r \cdot \cos\theta \cdot \cos t$.

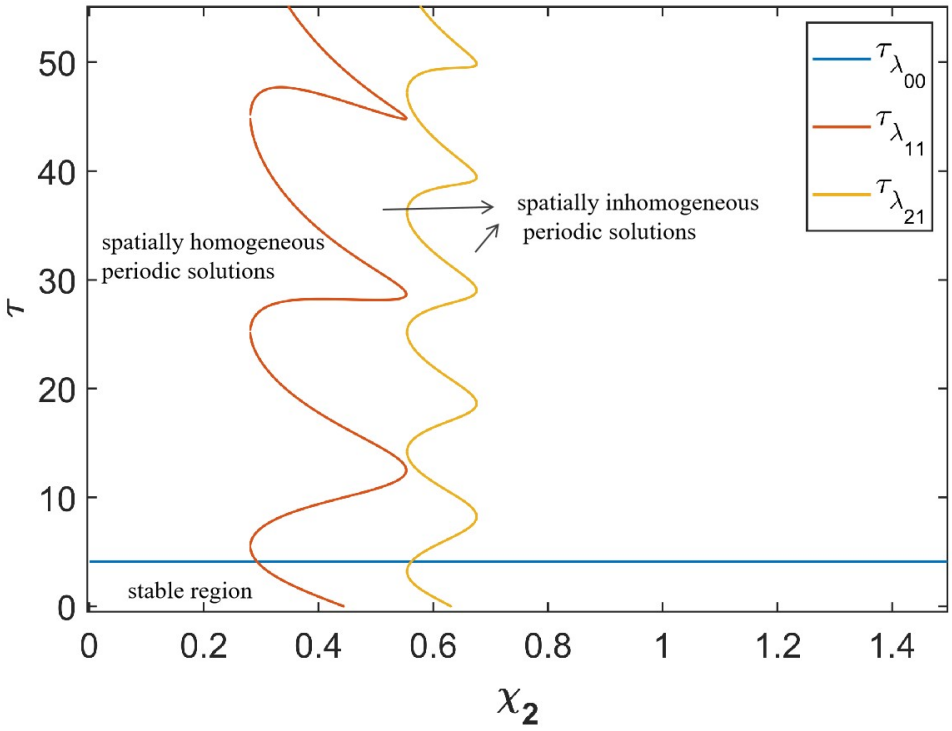

FIGURE 13. Partial bifurcation curves on the $\chi_2 - \tau$ plane. We choose $d_2 = 0.001$, and other parameter values that are given in (ii).

coefficient χ_2, the system gives rise to spatially inhomogeneous periodic solutions. From an ecological perspective, this corresponds to a scenario where non-toxic phytoplankton experience sustained but non-catastrophic grazing pressure, potentially establishing a classic predator–prey oscillatory dynamic with the zooplankton population. Under these conditions, the toxic phytoplankton population remains moderately controlled. Their toxin production offers protection yet does not guarantee absolute safety; they can coexist with the non-toxic type but typically do not achieve absolute dominance. For the zooplankton population, this state is the most stable and sustainable, as it provides flexibility in food sources—relying on toxic phytoplankton as a backup when non-toxic prey is scarce—while keeping the risk of intoxication at a relatively low level. Such dynamics facilitate the long-term coexistence of all three populations, which is mathematically reflected in the stable spatially inhomogeneous periodic solutions we obtained.

5. Conclusion

In this paper, an NTP–TPP–zooplankton model with predater-taxis and time-delayed is considered. By means of bifurcation analysis and numerical simulation, the dynamic properties of the model are studied on a two-dimensional disk. Many interesting results are obtained.

In mathematics, the global existence and boundedness of the positive steady-state solution of the model are analyzed, and the conditions for the existence of Hopf bifurcation and equivariant Hopf bifurcation are given by selecting time delay as the bifurcation parameter. In addition, we calculate the normal form of the equivariant Hopf bifurcation and numerically simulate with the normal form coefficients. According to the expressions of the bifurcation parameters, we draw the bifurcation curves of the taxic term coefficient of TPP and bifurcation parameters which are also very interesting and different from the two-population biological model. In different regions of the figure of bifurcation curves, the plankton model showed complex spatio-temporal dynamics,

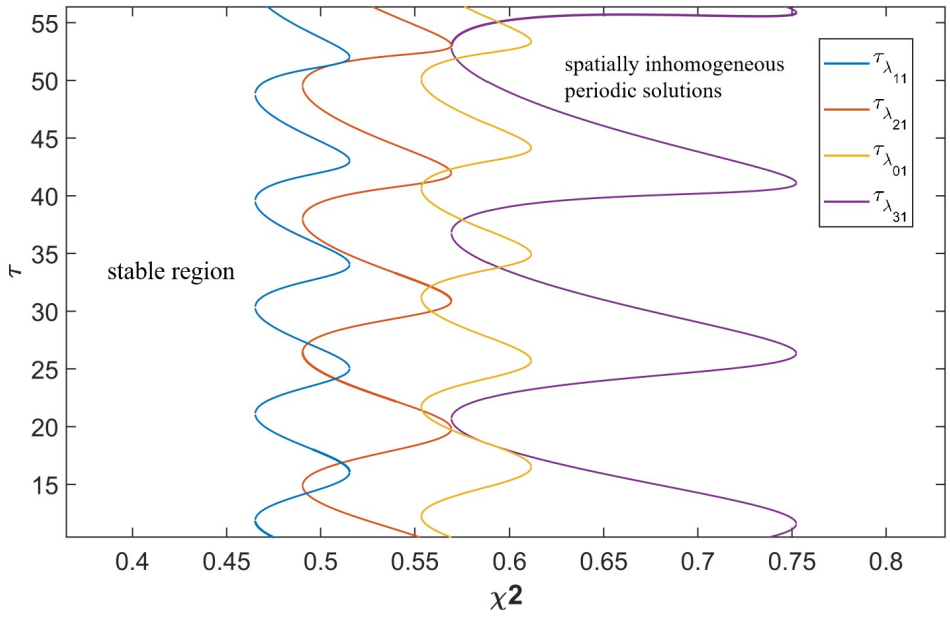

(a)

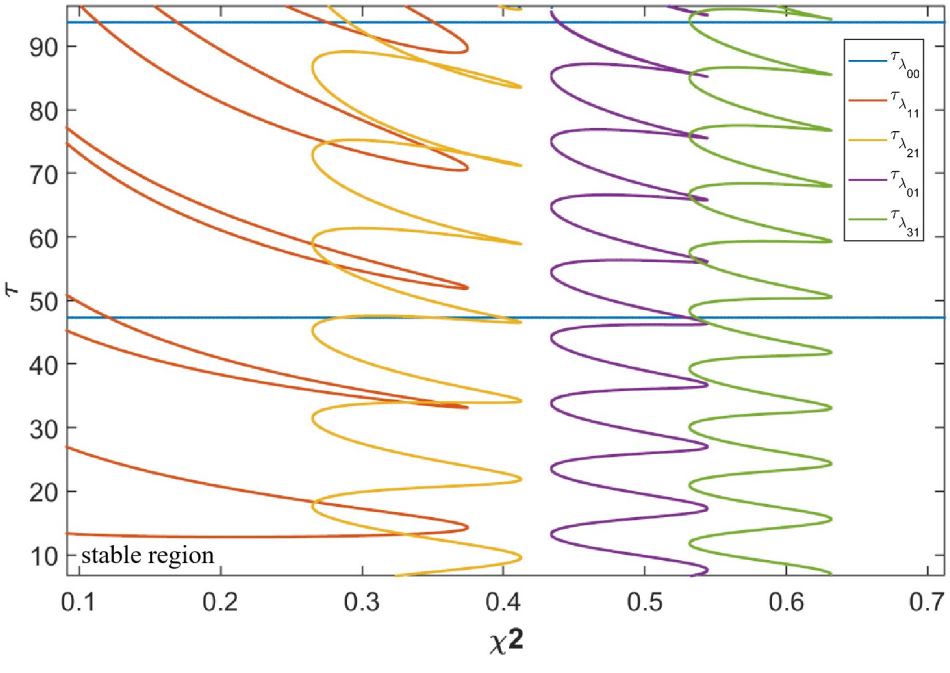

(b)

FIGURE 14. Partial bifurcation curves on the $\chi_2 - \tau$ plane. (a) We choose $A = 30$, $\delta = 0.7$, $D_1 = 0.1$, $D_2 = 0.5$, $D_3 = 0.4$, $\chi_1 = 0.05$, and other parameter values that are given in (ii), (b) We choose $A = 100$, $\delta = 0.1$, $D_1 = 0.8$, $D_2 = 0.1$, $D_3 = 0.5$, $\chi_1 = 0.17$, and other parameter values that are given in (ii).

including spatial homogeneous periodic solutions, different forms of rotating waves and standing waves, which are spatial non-homogeneous periodic solutions.

Ecologically, according to our simulations, it is intriguing to see how changes in the cannibalism coefficient affect the dynamic behavior of the system, which we have explained in detail in the previous section. In addition, the selective grazing of toxin-producing phytoplankton by plankton stabilizes the system structure to a certain extent, in other words, it helps to maintain the stability of the water ecosystem. In order to reduce algae outbreaks caused by eutrophication, we can regulate the selective predation of phytoplankton by zooplankton, which is also a sustainable biological control method. Combining the Allee effect, additional food, cannibalism and selective grazing, through the analysis of the periodic solution of the model, we can find the periodic phenomena of NTP, TPP and zooplankton. And by the intervention of these biological phenomena (such as the strength of the Allee effect, the amount of additional food, the level of cannibalistic competition, the degree of preference for NTP and the degree of avoidance of TPP and so on) we can realize the change and control of periodical phenomena, which is conducive to the management of aquatic ecological balance, and contribute significantly to many fields such as ecology, environmental science, fishery resource management and climate change research.

Funding

This work is supported by the Natural Science Foundation of Heilongjiang Province (No. LH2022A002) and the National Natural Science Foundation of China (No. 12371160).

Conflicts of interest

The authors have no conflicts to disclose.

Data availability statement

Data will be made available on request.

Author contribution statement

All authors participated in the writing and coordination of the manuscript and all authors read and approved the final manuscript.

References

[1] A.B. Medvinsky, *et al.*, Spatiotemporal complexity of plankton and fish dynamics. *SIAM Rev.* **44** (2002) 311–370.
[2] D.M. Anderson, Turning back the harmful red tide. *Nature* **388** (1997) 513–514.
[3] A. Oaten and W.W. Murdoch, Switching, functional response, and stability in predator–prey systems. *Am. Naturalist* **109** (1975) 299–318.
[4] A. Mitra and K.J. Flynn, Accounting for variation in prey selectivity by zooplankton. *Ecol. Model.* **199** (2006) 82–92.
[5] S. Gaucel and D. Pontier, How predator food preference can change the destiny of native prey in predator–prey systems. *Biol. Invasions* **7** (2005) 795–806.
[6] K.G. Porter, Selective grazing and differential digestion of algae by zooplankton. *Nature* **244** (1973) 179–180.
[7] B.W. Frost, Effects of size and concentration of food particles on the feeding behavior of the marine planktonic copepod *Calanus pacificus*. *Limnol. Oceanogr.* **17** (1972) 805–815.
[8] T. Kiørboe, Foraging mode and prey size spectra of suspension-feeding copepods and other zooplankton. *Mar. Ecol. Progr. Ser.* **558** (2016) 15–20.
[9] Q. Zhao, *et al.*, Dynamic behavior analysis of phytoplankton–zooplankton system with cell size and time delay. *Chaos Solitons Fractals* **113** (2018) 160–168.
[10] M.G. Danielsdottir, *et al.*, Phytoplankton food quality control of planktonic food web processes. *Hydrobiologia* **589** (2007) 29–41.

[11] X. Liu, *et al.*, Microzooplankton grazing and selective feeding during bloom periods in the Tolo Harbour area as revealed by HPLC pigment analysis. *J. Sea Res.* **90** (2014) 83–94.

[12] W.R. Demott, Optimal foraging theory as a predictor of chemically mediated food selection by suspension-feeding copepods. *Limnol. Oceanogr.* **34** (1989) 140–154.

[13] M. Schultz and T. Kiørboe, Active prey selection in two pelagic copepods feeding on potentially toxic and non-toxic dinoflagellates. *J. Plankton Res.* **31** (2009) 553–561.

[14] N.D. Lewis, *et al.*, Role of infochemical mediated zooplankton grazing in a phytoplankton competition model. *Ecol. Complex.* **16** (2013) 41–50.

[15] S.-i. Uye and K. Takamatsu, Feeding interactions between planktonic copepods and red-tide flagellates from Japanese coastal waters. *Mar. Ecol. Progr. Ser.* **59** (1990) 97–107.

[16] S.F. Sailley, *et al.*, Impact of zooplankton food selectivity on plankton dynamics and nutrient cycling. *J. Plankton Res.* **37** (2015) 519–529.

[17] K. Agnihotri and H. Kaur, Optimal control of harvesting effort in a phytoplankton-zooplankton model with infected zooplankton under the influence of toxicity. *Math. Comput. Simul.* **190** (2021) 946–964.

[18] J. Sole, *et al.*, The role of selective predation in harmful algal blooms. *J. Mar. Syst.* **62** (2006) 46–54.

[19] C.J. Gobler, Climate change and harmful algal blooms: insights and perspective. *Harmful Algae* **91** (2020) 101731.

[20] Y. Zheng, *et al.*, Selective grazing of zooplankton on phytoplankton defines rapid algal succession and blooms in oceans. *Ecol. Model.* **468** (2022) 109947.

[21] M.L. Rosenzweig, Paradox of enrichment: destabilization of exploitation ecosystems in ecological time. *Science* **171** (1971) 385–387.

[22] X. Meng and L. Zhang, Evolutionary dynamics in a Lotka–Volterra competition model with impulsive periodic disturbance. *Math. Methods Appl. Sci.* **39** (2016) 177–188.

[23] T. Zhang, *et al.*, Global dynamics of a model for treating microorganisms in sewage by periodically adding microbial flocculants. *Math. Biosci. Eng.* **171** (2019) 179–201.

[24] N.K. Thakur, *et al.*, Diffusive three species plankton model in the presence of toxic prey: application to Sundarban mangrove wetland. *J. Biol. Syst.* **25** (2017) 185–206.

[25] S. Roy, *et al.*, Competing effects of toxin-producing phytoplankton on overall plankton populations in the Bay of Bengal. *Bull. Math. Biol.* **68** (2006) 2303–2320.

[26] S. Chakraborty, *et al.*, The role of avoidance by zooplankton for survival and dominance of toxic phytoplankton. *Ecol. Complex.* **11** (2012) 144–153.

[27] T. Vrede and K. Vrede, Contrasting "top-down" effects of crustacean zooplankton grazing on bacteria and phytoflagellates. *Aquat. Ecol.* **39** (2005) 283–293.

[28] R. Rani and S. Gakkhar, The impact of provision of additional food to predator in predator–prey model with combined harvesting in the presence of toxicity. *J. Appl. Math. Comput.* **60** (2019) 673–701.

[29] L.R. Fox, Cannibalism in natural populations. *Annu. Rev. Ecol. Evol. Syst.* **6** (1975) 87–106.

[30] P. Mishra, *et al.*, On a cannibalistic predator–prey model with prey defense and diffusion. *Appl. Math. Model.* **90** (2021) 165–190.

[31] F. Courchamp, *et al.*, Allee effects in ecology and conservation. *J. Mammal.* **91** (2008) 1530–1532.

[32] R. Han, *et al.*. Spatio-temporal pattern selection in a prey–predator model with hunting cooperation and allee effect in prey. *SSRN Electr. J.* **171** (2023) 113441.

[33] S.O. Lehtinen, Ecological and evolutionary consequences of predator–prey role reversal: allee effect and catastrophic predator extinction. *J. Theoret. Biol.* **23** (2020) 110542.

[34] Y. Yang and M. Fan, Impact of selective grazing on the dynamics of a diffusive plankton model with component Allee effect and additional food. *Chaos Solitons Fractals* **175** (2023) 114004.

[35] R.M. Hillary and M. Bees, Plankton lattices and the role of chaos in plankton patchiness. *Phys. Rev. E Statist. Nonlinear Soft Matter Phys.* **69** (2004) 031913.

[36] N.M. Macdonald, Time lags in biological models. *Lect. Notes Biomath.* **27** (1978) 96–125.

[37] Y. Xia, *et al.*, Global analysis and optimal harvesting for a hybrid stochastic phytoplankton–zooplankton–fish model with distributed delays. *Math. Biosci. Eng.* **17** (2020) 6149–6180.

[38] Z. Jiang, *et al.*, Bifurcation and control of a planktonic ecological system with double delays by delayed feedback control. *J. Franklin Inst.* **358** (2021) 3609–3632.

[39] K. Das and S. Ray, Effect of delay on nutrient cycling in phytoplankton–zooplankton interactions in estuarine system. *Ecol. Model.* **215** (2008) 69–76.
[40] S.R.-J. Jang and J. Baglama, Nutrient-plankton models with nutrient recycling. *Comput. Math. Appl.* **49** (2005) 375–387.
[41] Y. Chen, *et al.*, Equivariant Hopf bifurcation in a class of partial functional differential equations on a circular domain. *Int. J. Bifurc. Chaos Appl. Sci. Eng.* **34** (2023) 2450079:1–2450079:19.
[42] Y. Chen, *et al.*, Equivariant Hopf bifurcation arising in circular-distributed predator–prey interaction with taxis. *Nonlinear Dyn.* **112** (2024) 12667–12675.
[43] S. Gakkhar and R.K. Naji, Chaos in three species ratio dependent food chain. *Chaos Solitons Fractals* **14** (2002) 771–778.
[44] A. Sharma, *et al.*, Complex dynamic of plankton–fish interaction with quadratic harvesting and time delay. *Model. Earth Syst. Environ.* **2** (2016) 1–17.
[45] N.K. Thakur, *et al.*, Harmful algal blooms in fresh and marine water systems: the role of toxin producing phytoplankton. *Int. J. Biomath.* **9** (2016) 1650043.
[46] T.R. Mohanty, *et al.*, Diel variation of plankton in the highly impacted freshwater zone of Hooghly estuary in relation to ecological alteration. *Environ. Monitor. Assessment* **196** (2024) 154.
[47] A. Mandal, *et al.*, Seasonal refuge patterns of phytoplankton trigger irregular bloom events in a contaminated environment. *Sci. Rep.* **14** (2024) 25248.
[48] A.B. Medvinsky, *et al.*, Direct input of monitoring data into a mechanistic ecological model as a way to identify the phytoplankton growth-rate response to temperature variations. *Sci. Rep.* **13** (2023) 10124.
[49] H. Amann, Dynamic theory of quasilinear parabolic equations. II. Reaction–diffusion systems. *Differ. Integral Equ.* **3** (1990) 13–75.
[50] H. Amann, Nonhomogeneous linear and quasilinear elliptic and parabolic boundary value problems. *Funct. Spaces Differ. Oper. Nonlinear Anal.* **133** (1993) 9–126.
[51] D. Horstmann and M. Winkler, Boundedness vs. blow-up in a chemotaxis system. *J. Differ. Equ.* **215** (2005) 52–107.
[52] M. Winkler, Aggregation vs. global diffusive behavior in the higher-dimensional Keller–Segel model. *J. Differ. Equ.* **248** (2010) 2889–2905.
[53] A. Friedman, Partial differential equations of parabolic type. *Operator Theory Adv. Appl.* **148** (1983) 77–113.
[54] M. Winkler and K. Djie, Boundedness and finite-time collapse in a chemotaxis system with volume-filling effect. *Nonlinear Anal. Theory Methods Appl.* **72** (2010) 1044–1064.
[55] D. Geng, *et al.*, Double-Hopf bifurcation and pattern formation of a Gause–Kolmogorov-type system with indirect prey-taxis and direct predator-taxis. *Commun. Nonlinear Sci. Numer. Simul.* **128** (2023) 107647.
[56] J. Wang and X. Guo, Dynamics and pattern formations in a three-species predator–prey model with two prey-taxis. *J. Math. Anal. Appl.* **475** (2019) 1054–1072.
[57] N.K. Thakur, *et al.*, Dynamical study of harmful algal bloom in Sundarban mangrove wetland with spatial interaction and competing effects. *Model. Earth Syst. Environ.* **8** (2021) 555–577.
[58] S. Mondal and G. Samanta, Dynamics of an additional food provided predator–prey system with prey refuge dependent on both species and constant harvest in predator. *Physica A Statist. Mech. Appl.* **534** (2019) 122301.

Please help to maintain this journal in open access!

This journal is currently published in open access under the Subscribe to Open model (S2O). We are thankful to our subscribers and supporters for making it possible to publish this journal in open access in the current year, free of charge for authors and readers.

Check with your library that it subscribes to the journal, or consider making a personal donation to the S2O programme by contacting subscribers@edpsciences.org.

More information, including a list of supporters and financial transparency reports, is available at https://edpsciences.org/en/subscribe-to-open-s2o.